



Beam Structure Design Analysis

Jordi Mata Garcia

Degree Thesis
Materials Processing Technology
2020

DEGREE THESIS	
Arcada	
Degree Programme:	Materials Processing Technology
Identification number:	7692
Author:	Jordi Mata Garcia
Title:	Beam Structure Design Analysis
Supervisor (Arcada):	Mathew Vihtonen
Commissioned by:	Arcada
<p>Abstract:</p> <p>A hypothetical scenario of a 30 m long, 10 m deep gap is proposed and a structure is to be created to allow pedestrians to cross it using not only the traditional beam analysis methods but also the standards and conventions proposed by the Eurocode 3 standard book, which have to be complied by the structures built within the European Union in order to be approved as safe. The structures must sustain a uniform applied load of 4 kN/m² as is the safety protocol for pedestrian bridges. A total of 3 different bridges constituted by I-shaped beams per the IPE profile standards, which is one of the most standardized profiles concerning bridge design specially concerning trusses, are proposed and verified through the European standards: a simply supported bridge with 2 sections of 2 supports evenly spaced out, a simple cantilever bridge with a single support base with two columns, and a Truss bridge separating the 30 m into 6 sections of 5 m long by 5 m high squares. All the bridges have the same 10 m x 4 m bridge deck in common, with 3 supporting beams. The initial profiles on the bridges and the deck rendered by the traditional method of analysis are then progressively increased to fulfil the standards established. A final choice of IPE450 beams for the bridge deck, IPE300 for the simply supported bridge columns, IPE600 for the simple cantilever bridge and IPE300 for the truss bridges are selected, all of them verified also through FEA analyses using COMSOL and SolidWorks software tools in order to obtain a Factor of Safety rating above 3.0 in all the members of the structure. The simulation task brought up the high potential and considerations of the European standards, as the beams had enough capabilities not only to conform to a very solid and stable structure but also to withstand the effect of gravity on the structure. No bridge option was markedly better than the next one in terms of stability, each of them having its benefits concerning the supporting system depending on the terrain conditions: simply supported bridge in case there is an obstacle in the centre of the gap, simple cantilever bridge if it is the support that must be located in the centre, truss bridge in case a supporting structure is not a feasible option.</p>	
Keywords:	Structural analysis, FEA analysis, beam structure, structural design, COMSOL, SolidWorks
Number of pages:	63
Language:	English
Date of acceptance:	

CONTENTS

1	Introduction.....	11
1.1	Relationship to existing knowledge	12
1.2	Relevance of the problem	12
2	Literature Review	13
2.1	Determinate structures	13
2.1.1	<i>Loads.....</i>	<i>13</i>
2.1.2	<i>Deflections.....</i>	<i>15</i>
2.2	Indeterminate structures.....	16
2.2.1	<i>Displacement method of analysis.....</i>	<i>17</i>
2.2.2	<i>Approximate method</i>	<i>19</i>
2.2.3	<i>Stiffness method.....</i>	<i>20</i>
2.3	Beam failure types.....	22
2.4	Beam design according to European standards	23
2.4.1	<i>Beam's geometry analysis and material properties</i>	<i>23</i>
2.4.2	<i>Load analysis and maximum deflection permitted</i>	<i>25</i>
2.4.3	<i>Resistance verification.....</i>	<i>27</i>
2.4.4	<i>Members in compression</i>	<i>31</i>
3	Method.....	34
3.1	Scenario proposal.....	34
3.2	Proposed solutions and initial analyses	35
3.2.1	<i>Bridge deck design</i>	<i>35</i>
3.2.2	<i>Simply supported bridge.....</i>	<i>37</i>
3.2.3	<i>Simple cantilever bridge</i>	<i>38</i>
3.2.4	<i>Truss bridge.....</i>	<i>39</i>
3.2.5	<i>Failure analysis applied to the critical components.....</i>	<i>40</i>
3.2.6	<i>Summary of beam profile selection according to Eurocode 3.....</i>	<i>44</i>
3.3	COMSOL Methodology	45
4	Results	46
4.1	Bridge deck.....	46
4.2	Simple bridge.....	49
4.3	Simple cantilever bridge	51
4.4	Truss bridge.....	52
4.5	Result comparison on minimum beam profiles	53
5	Discussion	53

5.1	Limitations	53
5.2	Bridge deck.....	54
5.3	Simply supported bridge.....	55
5.4	Simple cantilever bridge	55
5.5	Truss bridge.....	55
6	Conclusions	56
	References	57
	Appendix A.....	58
	Appendix B.....	59
	Appendix C.....	61
	Appendix D.....	62

Figures

Figure 1. Cable differential segment free-body diagram. Adapted from [1, Fig. 5-3]	14
Figure 2. Cross-section notations	23
Figure 3. Recommended limiting values for vertical deflections from ENV 1993-1-1. [3, Table 7.1]	26
Figure 4. Correction factors k_c . [3, Table 7.5]	30
Figure 5. Members under compression to European standards flow chart. (Jordi Mata Garcia, 2021)	33
Figure 6. Beam design according to European standards flow chart. (Jordi Mata Garcia, 2021)	33
Figure 7. Weight distribution on a one-way slab system. Adapted from [1, fig.2-11(b)]	35
Figure 8. Deck's central beam ideal representation. (Jordi Mata Garcia, 2021)	36
Figure 9. Deck girder-beam ideal representation. (Jordi Mata Garcia, 2021)	36
Figure 10. Bridge deck 3D design. Dimensions in meters. (Jordi Mata Garcia, 2021)	36
Figure 11. Simply supported bridge representation. (Jordi Mata Garcia, 2021)	37
Figure 12. Simple cantilever bridge representation. (Jordi Mata Garcia, 2021)	38
Figure 13. Cantilever column forces. (Jordi Mata Garcia, 2021)	38
Figure 14. Pratt truss bridge design. (Jordi Mata Garcia, 2020)	39
Figure 15. Pratt truss bridge design with forces. Red is compression, blue is tension. (Jordi Mata Garcia, 2020)	39
Figure 16. Bridge deck - Torsional moment analysis in COMSOL. (Jordi Mata Garcia, 2021)	47
Figure 17. Bridge deck – first principal stress analysis in COMSOL (Jordi Mata Garcia, 2021).	47
Figure 18. Bridge deck - Normal stress analysis in COMSOL (Jordi Mata Garcia, 2021).	48
Figure 19. Bridge deck - von Mises stress analysis in COMSOL (Jordi Mata Garcia, 2021).	48
Figure 20. Simply supported bridge - whole structure von Mises stress analysis with equal loads in COMSOL. Deformation scaled by 150x. (Jordi Mata Garcia, 2021)	49

Figure 21. Bridge deck - whole structure von Mises stress analysis with middle-span load increased by 1.5x in COMSOL. Deformation scaled by 150x. (Jordi Mata Garcia, 2021)	50
Figure 22. Simply supported bridge. (Jordi Mata Garcia, 2021)	50
Figure 23. Simple cantilever bridge - whole structure von Mises stress analysis with equal loads. Deformation scaled by 200x. (Jordi Mata Garcia, 2021)	51
Figure 24. Simple cantilever bridge. (Jordi Mata Garcia, 2021)	51
Figure 25. Truss bridge von Mises analysis in COMSOL. (Jordi Mata Garcia, 2021)	52
Figure 26. Truss bridge. (Jordi Mata Garcia, 2021)	52

Tables

Table 1. Real to conjugated beam conversions. Adapted from [1, Table 7.2]	16
Table 2. Moment Distribution table example.	18
Table 3. An example table of the beam's geometry and material properties	23
Table 4. Cross-section classification table	25
Table 5. Classification summary table. Adapted from EN 1993-1-1: Table 5.2. [3, eq. (7.16a-d)]	25
Table 6. Minimum geometrical characteristics of cross-sections.	26
Table 7. Recommended values for lateral torsional buckling curves. Adapted from [3, Tables 7.2-7.4].	30
Table 8. Stability curve and imperfection factor in compression. Adapted from [3, Table 6.3a] and [2, Table 6.1].	32
Table 9. Profile - stresses traditional analyses. (Jordi Mata Garcia, 2021)	41
Table 10. Result comparison on minimum beam profiles between Eurocode 3 and COMSOL.	53

ABBREVIATIONS

Abbreviation	Definition	Unit
F	Force	N
P	Point Load	N
W	Distributed Load	N/m
V	Shear Force	N
M	Internal Moment	$N \cdot m$
T	Tensile Force	N
DOF	Degrees of Freedom	—
A	Area of Cross-Section	m^2
E	Young's Elastic Modulus	Pa
k	Span Stiffness	m^3
I	Second moment of Area / Moment of inertia	m^4
L	Length of Member	m
θ	Angular Displacement	rad
ψ	Angular Span Rotation	rad
Δ	Linear Displacement	m
FEM	Fixed-End Moment	$N \cdot M$
DF	Distribution Factor	—
CO	Carry-Over Factor	—
q	Local Loads	N
Q	Global Loads	N
d	Local Displacements	m
D	Global Displacements	m
T	Transformation Matrix	—
k'	Member Stiffness Matrix	m^3
K	Structure Stiffness Matrix	m^3

continued on next page

Abbreviation	Definition	Unit
r	Root Radius	m
h	Height	m
b	Width / Breadth	m
t_w	Thickness of Web	m
t_f	Thickness of Flange	m
I_t	Torsion Constant	m^4
I_w	Warping Constant	m^6
W_y	Section Modulus	m^3
ρ	Density	kg/m^3
ν	Poisson's ratio	—
f_y	Yield Strength	Pa
f_u	Ultimate Strength	Pa
G	Shear Modulus	Pa
α	Thermal Expansion Coefficient	$(^\circ C)^{-1}$
c	Flange-only breadth	m
d	Web-only Length	m
ε	Reduction Factor	$(Pa)^{-1}$
γ_M	Partial Safety Factor	—
δ	Beam Deflection	m
$V_{c,Rd}$	Design Shear Resistance	N
A_v	Shear Area	m^2
τ	Shear Stress Resistance	Pa
χ	Reduction Factor	—
ϕ	Reduction Factor Coefficient	—
$\bar{\lambda}$	Relative Slenderness	—

continued on next page

Abbreviation	Definition	Unit
C	Bending Moment Diagram Shape Coefficient	—
k_w	Warping Length End Factor	—
k_z	Restraint and Rotation Length End Factor	—
z_g	Load-Shear Centre Distance	m
z_j	Asymmetry Parameter	m
$N_{b,Rd}$	Column Buckling Available Strength	kN
N_{cr}	Elastic Critical Load	kN
N_{Ed}	Axial Load	kN

FOREWORD

I would first and foremost want to thank Mr Mathew Vihtonen, not only for suggesting to me the possibility of doing this thesis but also for trusting in my capabilities and letting me absolute freedom on how to approach the challenge, being it such a broad topic with many different possibilities.

This thesis also granted me the chance on exploring a rather unexplored terrain for me as structural stability and analysis. The possibility of being able to deeply understand and gain knowledge from Eurocode standards, understanding them and stretching their possibilities to suit the particular needs of certain situations has been not only inspiring but surprisingly entertaining to me. I often found myself lost in some readings concerning bridge construction, how to obtain the best possible stability with beam structures, not to mention the deep research I had the opportunity to do in software applications like SolidWorks and COMSOL that pushed my boundaries by a great extent.

At last, I would like to thank my family and friends whose support and trust through my studies could never go unnoticed, always helping my hand to reach farther than what I expected.

1 INTRODUCTION

The analysis of a steel structure consists of the determination of the different loadings and deflections that take place not only on a structure but in the structure member themselves [1, p. 19]. This analysis can be performed in numerous different ways, often requiring more than one study to be done in the same structure to find out the most efficient method and especially when trying to design a structure following a certain standard code.

Thus, comprehensive research concerning the aforementioned ways of analysing must be done when trying to assess a particular situation that may require the use of a structure, be it constituted by cantilevered or fixed beams, arches, cables, trusses, or several of them simultaneously focusing not only in both the structure as a whole and the different individual members but also on the joints and supports that bind them together. Once the structure has been deemed to be stable and its diverse loads and deflections determined, the individual beams and their joint connections have to be assessed to be considered safe to use.

Said beams may be shaped in different ways according to distinct standards around the world. In the matter of Europe, the European Committee for Standardisation developed ten European standards, named Eurocodes, concerning structural design [2]. In particular, Eurocode 3 (EN 1993) focuses on the design of steel structures and steel beams to determine whether they can withstand the design calculated loads and deflections within safety regulations against not only service-related failures but also environmental hazards or not [3]. As per the connections, the determination of their suitability and efficiency is crucial to ensure the best service of the structure.

These analysis combined will aid the engineer to achieve the most advisable structural design accounting not only for its safety, aesthetics, and serviceability but also for its economic and environmental constraints [1, p. 19].

1.1 Relationship to existing knowledge

On general terms, the analysis of structures is an important part of any materials engineering related degree as well as the strength of the materials used, among others. That is what could be referred to as the traditional method of analysis.

This method analyses structures following the basic principles of equilibrium, as structures are assumed to be stable in their functioning state in the majority of cases. Using this analysis it is possible to obtain an estimate on how certain applied loads translate to the rest of not only the member itself but also to the members of the structure. Then, the stresses produced can be extracted and compared as to whether the material can sustain it, but that comparison is unsuitable to most real-life structural applications since there are many other side-effects to be considered as to assess the safety of the member.

Hence, the insight offered by the traditional method must be expanded using either estimations or simulations of those side-effects. The European standards are the gateway to accomplish that task, and that is what this document will focus on.

1.2 Relevance of the problem

The traditional method of analysis will more often than not fail to reveal the true extent of a structure or a member's capability to withstand a certain applied load, let alone to environmental-originated forces or any sort of unexpected extra weight.

It is, then, crucial for any engineer not only to understand how a certain member can withstand the not-so-obvious forces created by the foregoing phenomena in order to deem that member as a safe part of a structure but as to be assess what are the required conditions said member must fulfil to be as cost-effective as possible for the viability of the structure. Understanding and mastering the European standards is, thus, a key milestone when it comes to structural analysis in real life.

2 LITERATURE REVIEW

When starting the design analysis process, the first step must always be to identify the elements constituting its shape and whether the analysed structure is either determinate or indeterminate to establish their loadings and deflections.

The determinacy of a structure depends on the number of reactions happening on it compared to the number of members. The stability of a member can be determined by the three equilibrium equations [1, Eq. (2-2)]:

$$\sum F_x = 0; \sum F_y = 0; \sum M_o = 0 \quad (1)$$

Thus, if the number of reactions in the structure is bigger than threefold the number of members of the structure will then be indeterminate. For a structure to be determinate the number of reactions must equal the total number of equilibrium equations in the structure.

2.1 Determinate structures

2.1.1 Loads

Loads in statically determinate structures can be analysed by applying Eq. (1). Said equations can be adapted under certain circumstances to ease the analysis by associating them to each other through the parameters present in some of the members. That is the case, for example, of cables and arches (a frequent element to help stabilize the total load on certain structures like bridges) or trusses.

Cables act in tension assuming they are perfectly flexible. When subjected to concentrated loads, it is safe to apply the equations of equilibrium (Eq. (1)) at either the joints that the applied loads create or the segments in-between them. In the event of an external distributed load being applied or the weight of the cable is taken into consideration, then the shape of the cable must be analysed as follows:

1. The origin of the x, y coordinate system is placed at the lowest point of the cable where the slope is zero. A differential segment of the cable is then taken into consideration analysing the forces acting there.
2. Taking that tensile force T through the cable's length s increases continuously along its angle θ , the free-body diagram shown in Figure 1 can be considered:

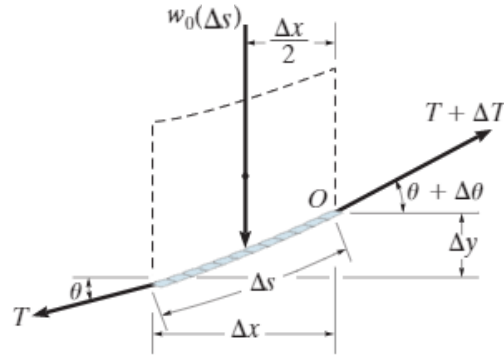


Figure 1. Cable differential segment free-body diagram. Adapted from [1, Fig. 5-3]

3. Eq. (1) when applying the limits $\Delta y \rightarrow 0$, $\Delta\theta \rightarrow 0$ and $\Delta T \rightarrow 0$ at $x = 0$, it is obtained through integration that:

- $T \cos \theta = F_x$ [1, eq. (5-4)]
- $T \sin \theta = \int w(s) ds$ [1, eq. (5-12)]
- $\tan \theta = dy/dx = (1/F_x) \int w(s) ds$ [1, eq. (5-13)]

The combination of these three equations yields the final parabolic equation [1, (eq. 5-14)]:

$$x = \int \frac{1}{\sqrt{1 + \frac{1}{F_x^2} (\int w(s) ds)^2}} ds \quad (2)$$

its two constants determined by applying the cable's boundary conditions.

It is important to observe also that the maximum value of the tension T can be obtained from observing the point of θ_{max} at $x = L$.

As per the arches, they are designed to work mainly in compression as opposed to cables. To support a uniform distribution of the load throughout its horizontal projection a parabolic shape is required, meaning that no bending or shear forces will occur within it: that arch shape is called a funicular arch [1, p. 220]. The equilibrium of forces is then calculated at each joint like previously.

Trusses, as noted by Hibbeler, are “structures composed of slender members joined together at their endpoints to form a series of triangles” [1, p. 152]. A pin connection supporting the member’s load is applied to every joint, hence creating either tension or compression in each of the members. The structure can then be analysed by either establishing equilibrium on its joints (method of joints), by assuming sections of the structure as solids and applying the equilibrium equations on their connecting joints (method of sections) or both methods simultaneously.

2.1.2 Deflections

The deflections in either the members of a structure or the structure themselves can be efficiently resolved once the moment diagram is known, as a positive moment (assuming positive as clockwise) will create a negative displacement (assuming positive as upwards) in the deflection curve and vice versa. This relationship works both ways, thus a known deflection curve will reveal the moment diagram easily. It is important to remember that the linear displacement Δ and the angular displacement θ on either joints or supports will depend on their type. No supports generally allow linear displacement yet pinned and roller supports allow an angular displacement while fixed supports do not; joints allow both of them, with the difference being that pin-connected joints create different angular displacements on the connected members while a fixed-connected joint does not. [1]

There are several methods to calculate the deflections happening on a beam like the double-integration method, the moment-area theorems, or the conjugate-beam method [1]. This last method will constitute the main method used in this study.

The conjugate-beam method consists of converting the analysed beam into a conjugate applying the transformations described in Table 1 [1, Table 7.2]. This method is based on the comparison between the real and the conjugate beam: a direct translation of the angular displacement on the real beam can be done to the shear in its conjugated form, and the same applies between the linear displacement on the real beam and the moment on the conjugated form. Thus, a normal analysis can be performed on the conjugated beam which will then render the displacements occurring in the real beam. As per the

loads, the M/EI diagram (that is the moment M over the member's flexural rigidity EI) of the real beam will be applied as a distributed load on the conjugated beam.

Table 1. Real to conjugated beam conversions. Adapted from [1, Table 7.2]

Real Beam		Conjugated Beam	
Pin support	θ $\Delta = 0$	Pin support	V $M = 0$
Roller support	θ $\Delta = 0$	Roller support	V $M = 0$
Fixed support	$\theta = 0$ $\Delta = 0$	Free end	$V = 0$ $M = 0$
Free end	θ Δ	Fixed support	V M
Internal pin	θ $\Delta = 0$	Hinge	V $M = 0$
Internal roller	θ $\Delta = 0$	Hinge	V $M = 0$
Hinge	θ Δ	Internal roller	V M

2.2 Indeterminate structures

As established previously, when the reactions exceed the total number of equilibrium equations in a structure it is then deemed indeterminate. The main goal is, then, to make the structure determinate to be suitable to be analysed. There are different methods to achieve that aim depending on the provided information, the placement of the members or the suitability of the methods themselves: the displacement method of analysis, the approximation analysis, and the stiffness method.

2.2.1 Displacement method of analysis

The displacement method of analysis consists, according to Hibbeler, of “writing the unknown displacements in terms of the loads using the load-displacement relationships” [1, p. 449] to achieve a determinate structure that can be analysed through the equilibrium equations. There are two main methods to accomplish that: using slope-deflection equations or using moment distribution.

2.2.1.1 Slope-deflection equations

Through the use of the slope-deflection equations, it is possible to conjoin the unknown moments happening at a specific joint of the structure to the unknown rotations (or degrees of freedom (DOF)) occurring in it. There are two different cases to be evaluated when applying the slope-deflection equations:

1. Far end of the member is fixed: the corresponding equation is applied to both ends of the member and is valid for either internal or end span [1, eq. (10-8)].

$$M_{NF} = 2Ek(2\theta_N + \theta_F - 3\psi) + (FEM)_N \quad (3)$$

where N and F are the assumed near and far end respectively, the span stiffness $k = I/L$, the angular span rotation $\psi = \Delta/L$ and FEM the Fixed-End Moments as described in Appendix A.

2. Far end of the member is either pin or roller supported: the corresponding equation is applied only at the near end [1, eq. (10-10)].

$$M_{NF} = 3Ek(\theta_N - \psi) + (FEM)_N \quad (4)$$

These equations are then substituted into the equations of moment equilibrium at each specific joint of the structure, leading to the solving of the unknown displacements. In the case of a frame structure having sidesway, where an unknown horizontal displacement takes place, the column shears are to be related to the moments at the joints and then solved in both the moment and force equilibrium equations.

2.2.1.2 Moment distribution

Another way of solving the DOF is the moment distribution method. It consists of successive approximations of locking and unlocking all the joints of the structure to allow the moment present in these to be distributed onto each connecting moment and carrying over half its value to the other side of the analysed span.

As a first step, all member stiffness factors are determined following four different cases:

- | | |
|--|-------------|
| 1. Far end is fixed [1, eq. (11-1)]: | $k = 4EI/L$ |
| 2. Far end is pinned or roller supported [1, eq. (11-4)]: | $k = 3EI/L$ |
| 3. Symmetric span and loading [1, eq. (11-5)]: | $k = 2EI/L$ |
| 4. Symmetric span but antisymmetric loading [1, eq. (11-6)]: | $k = 6EI/L$ |

Second, the distribution factors are found by dividing each member's stiffness factor by the total sum of the stiffness factors of the members present in the joint, also taking into consideration that the DF for a fixed end is $DF = 0$, and for a pin or roller-supported end is $DF = 1$. Finally, the Fixed-End Moments (see Appendix A) of each span must be calculated.

All the calculations can be easily quantized by using a Moment Distribution table as the one exemplified in Table 2:

Table 2. Moment Distribution table example.

Joint	A	B	C	D
Member				
DF				
FEM				
Distribution				
Carry-Over				
Distribution				
Carry-Over				

The Distribution and Carry-Over process (*CO*) must be repeated until a desired degree of accuracy is attained. Once this is reached, the moment at each joint is the sum of the moments from the cycle of locking and unlocking.

When a member in the structure has a non-prismatic shape, that is to say, a varying cross-section area along the member span, a variable moment of inertia also takes place during that same span. These members are often used on long-span structures to save material. Structural analysis of said members can be also executed using any of the methods mentioned before, slope-deflection equations or moment distribution.

To do this, it is needed to obtain the FEM of the members, as well as their stiffness (k) and carry-over (*CO*) factors. In the case of using the moment distribution analysis, the process can be then simplified further if the stiffness factor of one or several members is modified for the cases of end-span pin support, or structural symmetry or antisymmetry.

Even though the conjugate-beam method could be used, it is a very tedious work that could be simplified by using already tabulated data such as the one published by the Portland Cement Association [4].

2.2.2 Approximate method

The main objective of an approximate structural analysis is to reduce a statically indeterminate structure to one that is, thus, statically determinate. There are several methods of doing so:

- Trusses having cross-diagonal bracing within their structural panels can be analysed, given that the members are long and slender, by assuming that the tension diagonal supports the panel's shear and that the compression diagonal is a zero-force member. In case that the cross-section is larger, it is acceptable to assume that each diagonal member carries half of the panel's shear.
- An estimation can be made when analysing a girder of length L of a certain building frame as to assume that the girder does not support an axial load, and there are hinges located $0.1 L$ away from the supports.

- For portal frames with fixed supports, hinges are assumed at the midpoint of each column height (that is from the ground until the truss bracing). Each column is then assumed to support half the shear load on the frame, no matter if fixed or pin supported.
- For fixed and connected building frames subjected to a lateral load, the same hinge assumption at the centre of the columns can be made as well as the girder. Then, the analysis will depend on the frame elevation:
 - For low elevation, shear resistance is important and thus the portal method is used, where interior columns carry twice the shear as that of the exterior ones.
 - For tall and slender frames the cantilever method can be used, where the axial stress in a column is directly proportional to the distance from the cross-sectional area centroid of each column.

2.2.3 Stiffness method

When analysing structures with the use of a computer, the stiffness method is usually the way to go. This method requires numbering and plotting the coordinates of the elements and nodes for the entire structure taking the local coordinate system's origin at a selected near-end and establishing the global coordinates for the entire structure.

The first requirement is to formulate each member stiffness matrix in local coordinates (k'), relating the loads at the ends of the member (q) to their displacements (d) such as in $q = k'd$ [1, eq. (14-3)]. The stiffness matrix has the form of:

$$k' = \frac{AE}{L} \begin{bmatrix} 1 & -1 \\ -1 & 1 \end{bmatrix}$$

Next, the local displacements d are related to global displacements D through the transformation matrix T where $d = TD$ and, at the same time, local forces q are transformed into global forces Q using the same transformation matrix such as $q = TQ$. The transformation matrix has the form of:

$$T = \begin{bmatrix} \lambda_x & \lambda_y & 0 & 0 \\ 0 & 0 & \lambda_x & \lambda_y \end{bmatrix}$$

where $\lambda_x = (x_F - x_N)/L$ for each member and coordinate axis, being x_F and x_N the far and near end position on the x -axis.

When these matrices are finally combined, the result is the member's stiffness factor matrix $k = T^T \cdot k' \cdot T$, which is then assembled into the stiffness matrix K for the entire structure by superposition of all matrices k . The displacements and loads happening in the entirety of the structure are obtained through the partition of the equation $Q = KD$, which will be made as in [1, eq. (14-18)]:

$$\begin{bmatrix} Q_k \\ \dots \\ Q_u \end{bmatrix} = \begin{bmatrix} K_{11} & \vdots & K_{12} \\ \dots & \dots & \dots \\ K_{21} & \vdots & K_{22} \end{bmatrix} \begin{bmatrix} D_u \\ \dots \\ D_k \end{bmatrix} \quad (5)$$

where k stands for known variable, and u for unknown variable.

From equation 3, two equations can be obtained: $Q_k = K_{11}D_u + K_{12}D_k$ and $Q_u = K_{21}D_u + K_{22}D_k$. The combination of both will yield all unknown variables. Once those values have been calculated, each member's forces can be then obtained by combining $q = k'd$ and $d = TD$, thus: $q = k'TD$.

In a similar fashion as to analysing structures, the application of the stiffness method on beam analysis starts by identifying members and nodes, the latter being either supports or points where members are connected, where an external force is applied, where the cross-sectional area of the member suddenly changes or where a vertical or rotational displacement must be identified.

Then, a global and member coordinate system must be established paying attention that, unlike 0.with trusses, the global and member coordinates will be parallel due to their axis being collinear thus not needing to develop a transformation matrix.

Once the previous steps have been completed, the DOF can be then determined. Each node on a beam can have up to two degrees of freedom: a vertical displacement and a rotation. The lowest code numbers will be used to identify unknown displacements

(D_u). Being all the displacement correctly tagged, it is time to develop the stiffness matrix for each member according to its local coordinate system (x', y', z'), placing its origin at the selected near end N and extending the positive axis x' towards the far end F .

By applying the conjugate-beam method and superposing all the possible scenarios in equilibrium, the following stiffness matrix is obtained [1, eq. (15-1)]:

$$k = EI \cdot \begin{bmatrix} 12/L^3 & \frac{6}{L^2} & -\frac{12}{L^3} & \frac{6}{L^2} \\ 6/L^2 & \frac{4}{L} & -\frac{6}{L^2} & \frac{2}{L} \\ -12/L^3 & -\frac{6}{L^2} & \frac{12}{L^3} & -\frac{6}{L^2} \\ 6/L^2 & \frac{2}{L} & -\frac{6}{L^2} & \frac{4}{L} \end{bmatrix} \quad (6)$$

The superposition of the different member's stiffness matrix will then yield the stiffness matrix for the system K , which will then be used to determine the unknown loads and displacements happening in the system as in the previously used Equation 3 ($Q = KD$) and the local loads and displacements for each member as in $q = kd + q_0$ [1, eq. (15-5)], where q_0 represents the reversed fixed end loadings.

2.3 Beam failure types

To say that a beam is safe is the same as to say that a beam must avoid failing. There are different types of beam failure according to the different type of forces acting on it [5]:

1. Compression failure: when the axial load is higher than the load it was designed to sustain it results in a compression failure or buckling of the member.
2. Tension failure: if the tensile load acting on the member exceeds the resistance offered by the material strength, the member will fail.
3. Flexural failure: the combination of compressive and tensile forces acting on a beam due to the load applied can cause a twisting moment, that can result in the failure of the beam. That failure type is called lateral-torsional buckling.
4. Shear failure: if the shear load exceeds the shear value, the member will fail.

2.4 Beam design according to European standards

When a member undergoes bending moment, it is also affected generally by shear forces. These forces have to be considered as well as the beam's serviceability, that is deflections and other dynamic effects, resistance, and stability verifications. Thus, and according to Bernuzzi et al, it is "needed to evaluate some aspects related to the behaviour of the beam elements under flexure and shear". [3, p. 176]

When analysing a member to verify its accord with the Eurocode 3 European Standard, there are several steps to be followed.

2.4.1 Beam's geometry analysis and material properties

The very first phase of the study must start with the analysis of the beam's cross-section geometry and material properties. There exist several tables that collect the design properties of the different profiles and classes (see Appendix B). A table is then filled such as in the following example:

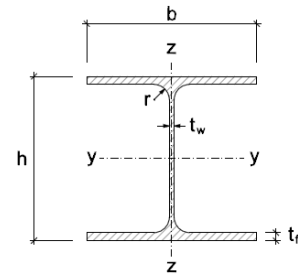


Table 3. An example table of the beam's geometry and material properties

Figure 2. Cross-section notations

r	Root radius	I_y	Moment of inertia about axis y-y
h	Height	I_z	Moment of inertia about axis z-z
b	Width/Breadth	I_t	Torsion constant
t_w	Web thickness	I_w	Warping constant
t_f	Flange thickness	$W_{el,y}$	Elastic section modulus about axis y-y
A	Area of the cross-section	$W_{pl,y}$	Plastic section modulus about axis y-y
L	Length of the beam	$L_{cr,LT}$	Critical length of the beam
S	Steel type (e.g. S275)	f_y	Yield strength
ρ	Density	f_u	Ultimate strength
E	Young's modulus	G	Shear modulus
ν	Poisson's ratio	α	Thermal expansion coefficient

Once all the data is gathered, the cross-section has to be classified into one of four classes [3, pp. 75, 109-110], the behaviour of which will determine the method to the analysis:

- Class 1, or plastic or ductile sections: These cross-sections provide an adequate rotational capacity for an effective plastic analysis without any reduction happening to its resistance.
- Class 2, or compact sections: These cross-sections, as the ones in class 1, provide a plastic moment resistance yet have limited rotational capacity due to local buckling.
- Class 3, or semi-compact sections: These cross-sections are capable of sustaining yielding stresses only in the more compressed fibres when an elastic stress distribution is taken into consideration due to local buckling impeding an adequate spread of the plasticity along the cross-section itself.
- Class 4, or slender sections: These cross-sections are subjected to local buckling in one or more parts of itself before yielding stress can be reached.

As per the methods of analysis, the following procedures can be adopted [3, pp. 76]:

- Elastic method (E): A linear elastic response can be safely assumed until the yielding stress is attained. This method can be used to analyse the four different classes, yet in the case of class 4, the effective geometrical properties of the cross-section must be referenced.
- Plastic method (P): A complete plasticity spread throughout the entire cross-section is assumed. This method can be used for the entirety of the class 1 evaluation and as an approach to evaluate the load-carrying capacity of class 1 and 2 cross-sections.
- Elasto-plastic method (EP): Simplified by an elastic-perfectly plastic relationship or with an elastic-plastic with strain hardening relationship, this method refers to the actual material constitutive law and can be applied in all 4 classes.

To establish to which class our beam belongs, the flanges and the web are looked at separately as shown in Table 4:

Table 4. Cross-section classification table

Flange	$c/(t_f)_{tot}$	Class: 1-4
Web	d/t_w	Class: 1-4
Section		Class: Take the worst class case.

where c is the breadth of only the flanges (that is excluding the thickness of the web and the root), $(t_f)_{tot}$ the total thickness of the flanges (that is both of them) and d the length of the web excluding both root and flange thicknesses.

The classes are determined according to the following:

Table 5. Classification summary table. Adapted from EN 1993-1-1: Table 5.2. [3, eq. (7.16a-d)]

	Flange	Web in bending	Web in compression	$M_{c,Rd}$
Class 1	$\leq 9\varepsilon$	$\leq 72\varepsilon$	$\leq 33\varepsilon$	$(W_{pl,y} \cdot f_y)/\gamma_{M0}$
Class 2	$\leq 10\varepsilon$	$\leq 83\varepsilon$	$\leq 38\varepsilon$	$(W_{pl,y} \cdot f_y)/\gamma_{M0}$
Class 3	$\leq 14\varepsilon$	$\leq 124\varepsilon$	$\leq 42\varepsilon$	$(W_{el,y} \cdot f_y)/\gamma_{M0}$
Class 4	Does not meet other requirements			$(W_{eff} \cdot f_y)/\gamma_{M0}$

where the reduction material factor $\varepsilon = \sqrt{235/f_y}$, $M_{c,Rd}$ stands for the moment capacity of the beam, W_{eff} stands for the effective elastic section modulus and γ_{M0} for the partial safety factor (see Table B3 in Appendix B)

2.4.2 Load analysis and maximum deflection permitted

Once the cross-section has been classified, the load W must be identified and correctly factorized in the event of dead (D) and live (L) loads taking place at the same time. There are two different approaches to the factorization of uniformly distributed loads according to Eurocode 0 [2]:

$$1. W = 1.35 W_D + 1.50 W_L \quad (7)$$

being this the most conservative approach. [4, eq. (6.10)]

- The higher value from either $W = 1.35 W_D + 1.05 W_L$ or $W = 1.25 W_D + 1.50 W_L$, the second one being the most used. [4, eq. (6.10a,b)]

Upon obtaining the value of the load, the maximum deflection permitted due to the total load δ_{max} is selected through the table shown in Figure 3 while the limit conditions [3, p. 229] have to be considered:

Table 6. Minimum geometrical characteristics of cross-sections.

Uniformly Distributed Loads	$\delta_{Lim} = \frac{5}{384} \cdot \frac{(W_D + W_L) \cdot L^4}{E \cdot I_{min}}$	$W_{min} = \frac{3}{2} \cdot \frac{(W_D + W_L) \cdot L^2}{8 \cdot f_y}$
Point-Placed Loads	$\delta_{Lim} = \frac{1}{48} \cdot \frac{(P_D + P_L) \cdot L^3}{E \cdot I_{min}}$	$W_{min} = \frac{3}{2} \cdot \frac{(P_D + P_L) \cdot L}{4 \cdot f_y}$
Evenly Spaced Point Loads	$\delta_{Lim} = \frac{23}{648} \cdot \frac{(P_D + P_L) \cdot L^3}{E \cdot I_{min}}$	$W_{min} = \frac{3}{2} \cdot \frac{(P_D + P_L) \cdot L}{3 \cdot f_y}$

Which can then help determine the minimum beam depth as [3, Eq. (7.147)]:

$$H_{min} = \frac{2I_{min}}{W_{min}} \quad (8)$$

Conditions	Limits	
	$\delta_{max} = \delta_1 + \delta_2 - \delta_0$	δ_2
Roofs generally	$\frac{L}{200}$	$\frac{L}{250}$
Roofs frequently carrying personnel other than for maintenance	$\frac{L}{250}$	$\frac{L}{300}$
Floors generally	$\frac{L}{250}$	$\frac{L}{300}$
Floors and roofs supporting plaster or other brittle finish or non-flexible partitions	$\frac{L}{250}$	$\frac{L}{350}$
Floors supporting columns (unless the deflection has been included in the global analysis for the ultimate limit states)	$\frac{L}{400}$	$\frac{L}{500}$
Where δ_{max} can impair appearance of the building	$\frac{L}{250}$	—

δ_0 = precamber (hogging) of the beam in the unloaded state (state 0)
 δ_1 = variation of the deflection of the beam due to permanent loads immediately after loading (state 1)
 δ_2 = variation of the deflection of the beam due to variable loading plus any time dependant deformations due to permanent load (state 2)

Figure 3. Recommended limiting values for vertical deflections from ENV 1993-1-1. [3, Table 7.1]

2.4.3 Resistance verification

2.4.3.1 Shear resistance

Direct analysis of the forces acting on the beam will render the maximum design shear force V_{Ed} . This design value at each cross-section must never be greater than the design shear resistance $V_{c,Rd}$, thus $V_{Ed} \leq V_{c,Rd}$ (7) [3, eq. (7.18)]. As to the calculation of the design shear resistance, the approach will vary depending on the method of analysis.

For plastic design, $V_{c,Rd}$ is then regarded as the design plastic shear resistance $V_{pl,Rd}$ and takes the form of:

$$V_{pl,Rd} = \frac{A_v \cdot f_y}{\sqrt{3} \cdot \gamma_{M0}} \quad (9)$$

where A_v is the shear area (see Appendix C for its adequate calculation), f_y is the yield strength and γ_{M0} is the partial safety factor (see Table B3 in Appendix B). [3, eq. (7.19)]

In the case of elastic design, to verify the design shear resistance in equation 7 the following criterion [3, eq. (7.20a,b)]:

$$\tau_{Ed} = \frac{V_{Ed} \cdot Q}{I \cdot t} \leq \frac{f_y}{\sqrt{3} \cdot \gamma_{M0}} \quad (10)$$

being τ_{Ed} the tangential shear stress, Q the first moment of the area above the examined point on the cross-section, I the moment of inertia of the whole cross-section and t the thickness at the examined point.

When the shear force is acting on a beam, in the event of the design shear force V_{Ed} being less than half of the plastic shear resistance $V_{pl,Rd}$ (as in $V_{ed} < 0.5 V_{pl,Rd}$) then its effect on the moment resistance is to be neglected unless if detected that the shear buckling reduces the resistance of the section (see Bending Resistance section). Otherwise, the reduced moment resistance should be based on reduced yield strength, $f_{y,red}$, obtained as [3, eq. (7.26-7.27a)]:

$$f_{y,red} = \left(1 - \left[\frac{2 \cdot V_{Ed}}{V_{pl,Rd}} - 1 \right]^2 \right) \cdot f_y \quad (11)$$

2.4.3.2 Bending resistance

As with the shear resistance, the design value of the bending moment, M_{Ed} , must satisfy the condition at each cross-section of $M_{Ed} \leq M_{c,Rd}$ (11) [3, eq. (7.16a)]. The moment capacity $M_{c,Rd}$ can be determined, depending on each class, according to Table 5.

In the event of shear buckling reducing the resistance of the section, the reduced design plastic resistance moment $M_{y,V,Rd}$ can be obtained, alternatively [3, eq. (7.28)], as:

$$M_{y,V,Rd} = \left(W_{pl,y} - \left[\frac{2 \cdot V_{Ed}}{V_{pl,Rd}} - 1 \right]^2 \frac{A_w^2}{4 \cdot t_w} \right) \cdot \frac{f_y}{\gamma_{M0}} \quad (12)$$

being A_w the area of the web cross-section.

2.4.3.3 Buckling resistance

When a beam is either properly restrained or has a certain type of cross-section, such as square or circular hollow sections, they are not very susceptible to lateral-torsional buckling by default [3, p. 190]. Happen the beam to fail these conditions, verification against the phenomenon is required. Thus, it must be guaranteed that $M_{Ed} \leq M_{b,Rd}$ (12)[3, eq. (7.29)] being M_{Ed} the design value of the moment and $M_{b,Rd}$ the design buckling resistance moment, which can be defined as [3, eq. (7.30)]:

$$M_{b,Rd} = \chi_{LT} \cdot W_y \cdot \frac{f_y}{\gamma_{M1}} \quad (13)$$

where χ_{LT} is the reduction factor for lateral-torsional buckling, W_y the class appropriate section modulus and γ_{M1} the safety coefficient (see Table C2 in Appendix C).

As to the calculation of the reduction factor χ_{LT} , two procedures can be applied: the general approach, or a more refined approach for doubly symmetrical I- / H-shaped profiles.

1. General Approach

The reduction factor is given by the following expression [3, eq. (7.31)]:

$$\chi_{LT} = \frac{1}{\phi_{LT} + \sqrt{\phi_{LT}^2 - \bar{\lambda}_{LT}^2}} \quad \text{being } \chi_{LT} \leq 1 \quad (14)$$

The term ϕ_{LT} being defined as [3, eq. (7.32)]:

$$\phi_{LT} = 0.5 \cdot [1 + \alpha_{LT}(\bar{\lambda}_{LT} - 0.2) + \bar{\lambda}_{LT}^2] \quad (15)$$

where α_{LT} is the imperfection factor corresponding to the appropriate buckling curve [3, p. 191] obtained as detailed in Table 7.

And the relative slenderness for lateral-torsional buckling $\bar{\lambda}_{LT}$ being defined as [3, (eq. 7.33)]:

$$\bar{\lambda}_{LT} = \sqrt{\frac{W_y \cdot f_y}{M_{cr}}} \quad (16)$$

where M_{cr} is the elastic critical moment for lateral-torsional buckling based on gross cross-sectional properties (see Equation (20)) [3, p. 191].

2. Method for I- / H- Shaped Profiles

The reduction factor is given by the following expression [3, eq. 7.34]:

$$\chi_{LT} = \frac{1}{\phi_{LT} + \sqrt{\phi_{LT}^2 - 0.75 \cdot \bar{\lambda}_{LT}^2}} \quad \text{being } \chi_{LT} \leq 1 \text{ and } \chi_{LT} \leq (1/\bar{\lambda}_{LT})^2 \quad (17)$$

The term ϕ_{LT} being defined as [3, eq. 7.35]:

$$\phi_{LT} = 0.5 \cdot [1 + \alpha_{LT}(\bar{\lambda}_{LT} - 0.4) + 0.75 \cdot \bar{\lambda}_{LT}^2] \quad (18)$$

And the relative slenderness defined as Equation (16).

If considering the moment distribution between the lateral restraints of the member, a factor f can be applied to the reduction factor as χ_{LT}/f [3, p. 193], defining the term f according to [2] as:

$$f = 1 - 0.5(1 - k_c) \left[1 - 2(\bar{\lambda}_{LT} - 0.8)^2 \right] \quad \text{being } f \leq 1 \quad (19)$$

where k_c is a correction factor depending on the moment distribution as according to Figure 4 [3, Tab. 7.5].

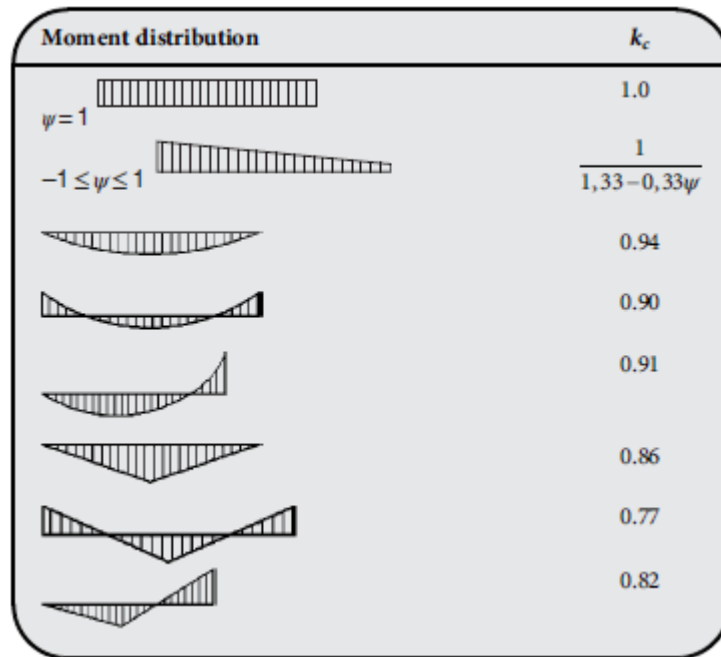


Figure 4. Correction factors k_c . [3, Table 7.5]

Table 7. Recommended values for lateral torsional buckling curves. Adapted from [3, Tables 7.2-7.4].

Stability curve	a	b	c	d
α_{LT}	0.21	0.34	0.49	0.76
GENERAL APPROACH:				
Cross-section	Limit		Stability curve	
Rolled I-sections	$h/b \leq 2$		a	
	$h/b > 2$		b	
Welded I-sections	$h/b \leq 2$		c	
	$h/b > 2$		d	
Other cross-sections	—		d	
METHOD FOR I-/H-SHAPED PROFILES				
Cross-section	Limit		Stability curve	
Rolled I-sections	$h/b \leq 2$		b	
	$h/b > 2$		c	
Welded I-sections	$h/b \leq 2$		c	
	$h/b > 2$		d	

The elastic critical moment M_{cr} can be calculated as [2, Annex F]:

$$M_{cr} = C_1 \frac{\pi^2 EI_z}{(k_z L)^2} \cdot \left\{ \left[\sqrt{\left(\frac{k_z}{k_w}\right)^2 \frac{I_w}{I_z} + \frac{(k_z L)^2 GI_t}{\pi^2 EI_z} + (C_2 z_g - C_3 z_j)^2} \right] - (C_2 z_g - C_3 z_j) \right\} \quad (20)$$

where C_1, C_2, C_3 are bending moment diagram shape-dependant coefficients, k_w and k_z are the effective length factors that deal with warping end restraint and rotation, z_g is the distance between the load application point and the shear centre or neutral axis and z_j is an asymmetry parameter [3, Eq. (7.39)].

For further calculation details for either the elastic critical moment or its parameters, refer to [3, pp. 193-199].

2.4.4 Members in compression

For the case of members working predominantly in compression, as is the case of columns, it is necessary to assess its column buckling available strength ($N_{b,Rd}$) to determine the safety of the element.

The first step after the correct classification of the cross-section according to its axial loading is to determine the elastic critical buckling load (N_{cr}) [3, Eq. (6.3)] about both its strong and weak axes as follows:

$$N_{cr} = \frac{\pi^2 EI}{L_o^2} \quad (21)$$

where L_o stands for the unbraced member length along the studied axis.

Once the elastic critical buckling stress has been determined, the relative slenderness $\bar{\lambda}$ [3, Eq. (6.26)] of each of the member's axes can be evaluated as:

$$\bar{\lambda} = \sqrt{\frac{A \cdot f_y}{N_{cr}}} \quad (22)$$

Note: For class 4 sections, A_{eff} [3, pp. 116,117] is to be used instead of A .

Using Table 8 the stability curve of the section is obtained alongside an imperfection factor α :

Table 8. Stability curve and imperfection factor in compression. Adapted from [3, Table 6.3a] and [2, Table 6.1].

Stability curve		a0	a	b	c	d
α		0.13	0.21	0.34	0.49	0.76
Hot-rolled I sections:						
Limit		Axis	Stability curve			
			S 460	Other steels		
$h/b > 1.2$	$t_f \leq 40 \text{ mm}$	y-y	a0	a		
		z-z	a0	b		
	$40 \text{ mm} \leq t_f \leq 100 \text{ mm}$	y-y	a	b		
		z-z	a	c		
$h/b \leq 1.2$	$t_f \leq 100 \text{ mm}$	y-y	a	b		
		z-z	a	c		
$t_f > 100 \text{ mm}$		y-y	c	d		
		z-z	c	d		

Being the stability curve correctly classified, a reduction factor χ can be calculated as previously formulated in Equations 14 and 15. Thus, with that reduction factor an available column buckling strength $N_{b,Rd}$ value can be obtained as follows:

$$N_{b,Rd} = \chi \cdot A \frac{f_y}{\gamma_{M1}} \quad (23)$$

Note: For class 4 sections, A_{eff} [3, pp. 116,117] is to be used instead of A .

Safety is then verified when both conditions $N_{cr} > N_{Ed}$ (24) and $N_b > N_{Ed}$ (25) are true for the member's weakest axis.

It is important to note that the buckling effect (thus, the verification of N_b) can be neglected if either $\bar{\lambda} \leq 0.2$ (26) or $N_{Ed}/N_{cr} \leq 0.04$ (27) happens to be true.

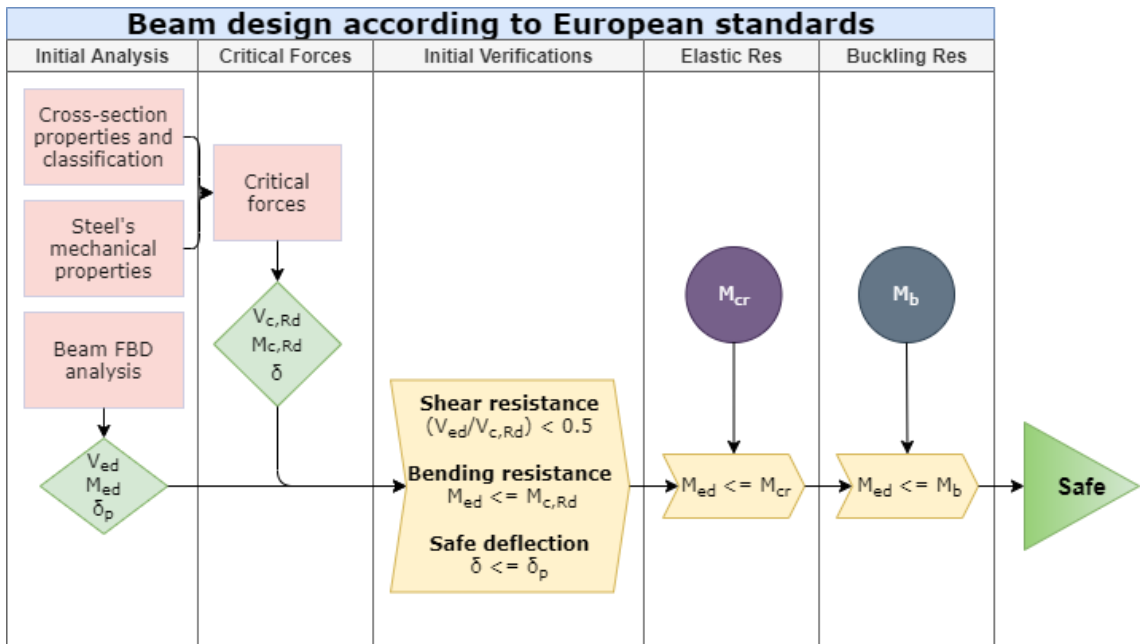


Figure 5. Beam design according to European standards flow chart. (Jordi Mata Garcia, 2021)

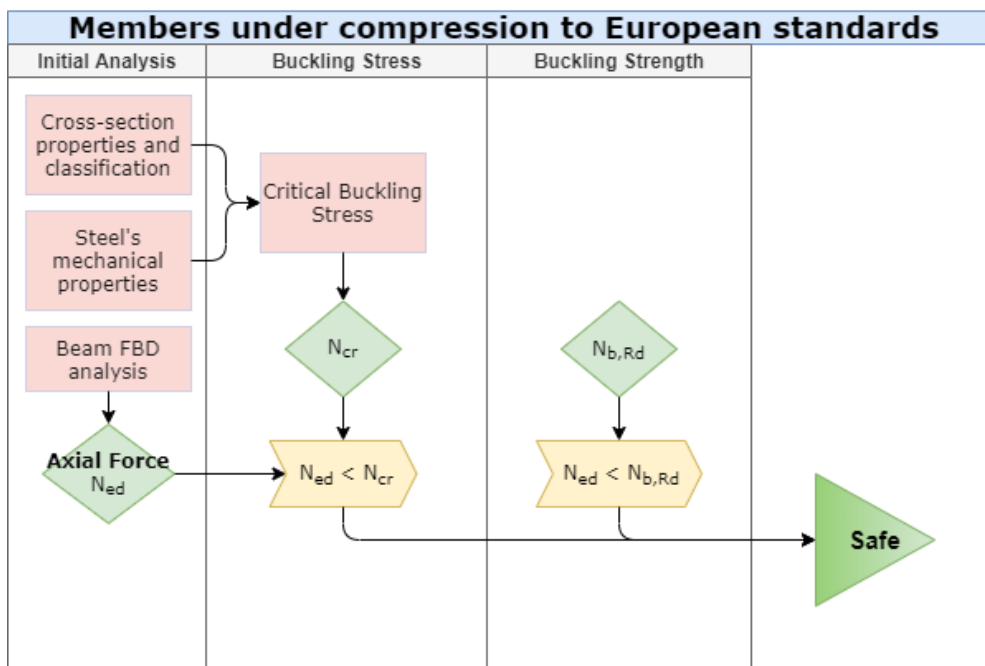


Figure 6. Members under compression to European standards flow chart. (Jordi Mata Garcia, 2021)

3 METHOD

The method to study the applications of the diverse analytic techniques reviewed in the previous chapter will be as follows:

1. A scenario will be proposed and the possible solutions suggested accordingly.
2. The traditional method of analyses will be conducted to determine the design values affecting the structure such as shear forces, moments, stresses, among many others.
3. Then, regulations established in the European standards on how structural design should be conducted within the European Union will be applied to each structural component to determine the ultimate safety of the structure.
4. Each structure will then be designed and analysed using computer software. Main results will be compared and studied concerning the individual suitability of each method in the specified scenario.
5. An estimation of the most suitable solution will be conducted, and discussion will be made on how to improve each design and on what factors could contribute to the selection of one solution over another.

3.1 Scenario proposal

The following scenario is considered:

- A structure is needed to allow pedestrians to cross over a gap, sized 30 meters long and 10 meters deep. Thus, the required structure is a bridge.
- The safety measures concerning pedestrian bridge loads [5] indicate that a pedestrian bridge must hold a total live load of 4 kN/m^2 . The dead and resulting total load will be calculated and the profiles readjusted through simulation.
- There are no constraints concerning the number of columns required, their placement or the distance. They will be adapted according to the bridge design specifications.
- A common bridge deck will be used for all bridges, consisting of three platforms sized $10 \text{ m} \times 4 \text{ m}$. Each platform will be composed of three evenly spaced lon-

gitudinal supporting beams, while the girders will be placed according to the support placement requirements.

- Beam cross-sections will be restrained to I-shaped beams for all the beams present in the structure, while its dimensions will depend entirely on the safety conditions established by the Eurocode 3 analyses.
- Structural reinforcement will be ignored by reason of pure beam analysis. Fasteners/bolts and welded joints will be assumed as perfect with higher resistance to failing than the beam members.

3.2 Proposed solutions and initial analyses

Three different structures are suggested to tackle the given scenario each of them requiring a different approach to be analysed: simply supported beam bridge, simple cantilever bridge and truss bridge.

3.2.1 Bridge deck design

The bridge deck used by all the different bridge designs consist of a thin $10\text{ m} \times 4\text{ m}$ metal plate to serve as a surface for the live load, three longitudinal beams of 10 m length that will carry the main weight of the thin plate and two or three 4 m long beams to act as girders on each end and placed below the beams depending on the situation.

This will create a one-way slab system [1, p. 58] that will distribute the load as shown in Figure 7 being so that the dark grey area will be the load supported by the central beam, represented as CD in the figure, and the rest of it distributed evenly to the side beams AB and EF. It is then observable that the central beam will be the critical component from the bridge deck structure as it will have to support 8 kN/m while the side beams will support half the amount.

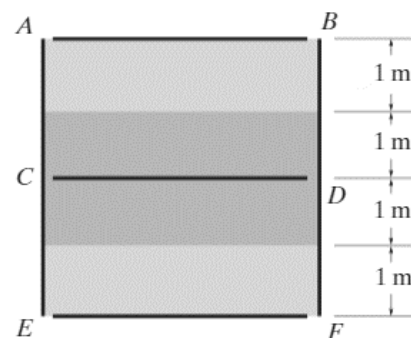


Figure 7. Weight distribution on a one-way slab system. Adapted from [1, fig.2-11(b)]

Thus, the central beam can be represented as:

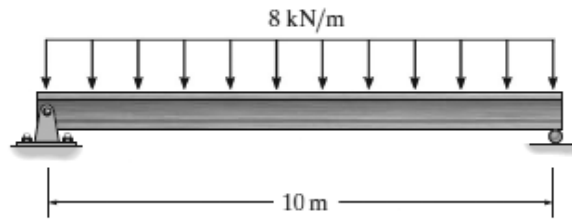


Figure 8. Deck's central beam ideal representation. (Jordi Mata Garcia, 2021)

The maximum design shear force V_{ed} and moment M_{ed} can then be calculated as $V_{ed} = \frac{8\text{ kN/m} \cdot 10\text{ m}}{2} = 40\text{ kN}$ and $M_{ed} = \frac{8\text{ kN/m} \cdot (10\text{ m})^2}{8} = 100\text{ kN} \cdot \text{m}$.

According to the aforementioned one-way slab system, it is manifest that the shear and moment forces acting on the side beams will be half of those acting on the central beam.

Like so, the girder beams could be represented as:

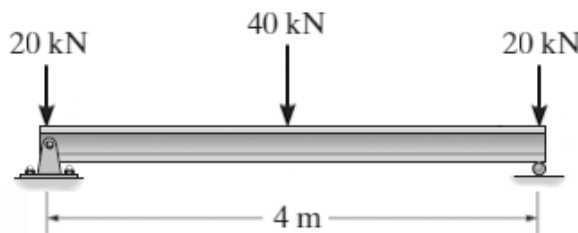


Figure 9. Deck girder-beam ideal representation. (Jordi Mata Garcia, 2021)

Which will produce a maximum shear of $V_{ed} = 40\text{ kN}$ and moment of $M_{ed} = 40\text{ kN} \cdot \text{m}$ on the beam. Despite this direct analysis not being accurate for every bridge model as it will depend on the column placement, it is the worst-case scenario when assuming evenly spaced supports.

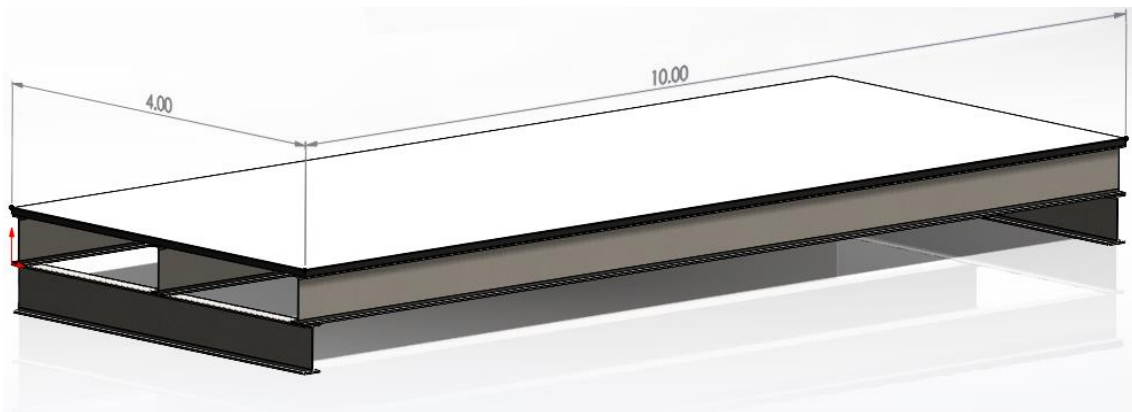


Figure 10. Bridge deck 3D design. Dimensions in meters. (Jordi Mata Garcia, 2021)

3.2.2 Simply supported bridge

On an initial investigation and due to the deck spans being 10 m long, the most logical column placement is at the union of said spans thus resulting in two-column joints as depicted in Figure 11.

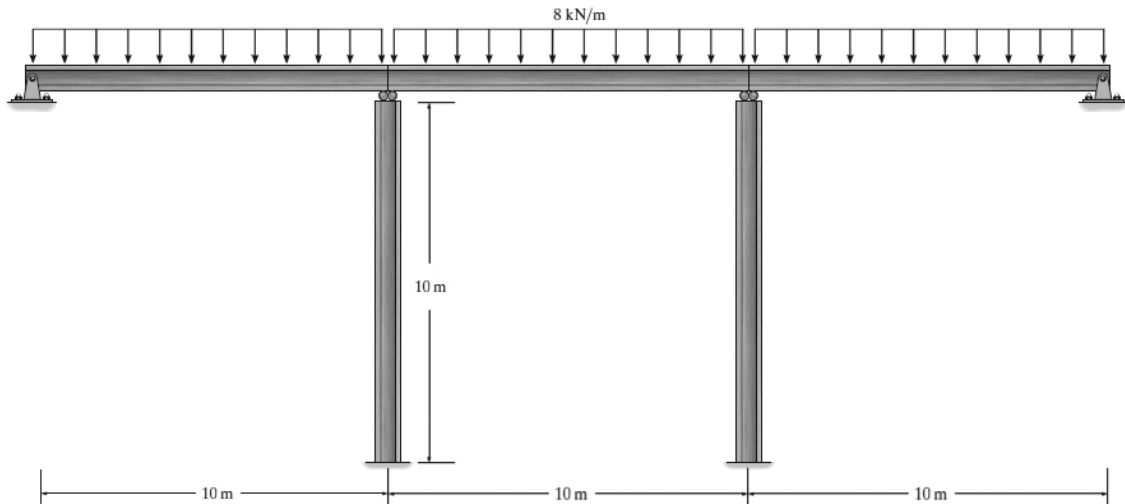


Figure 11. Simply supported bridge representation. (Jordi Mata Garcia, 2021)

At each column joint, there are then different possibilities concerning the number of supporting members. Being the deck light material-wise due to it being a pedestrian bridge it is safe to assume that both the environmental forces and the live loads traversing it will create a considerable rocking motion effect on the platform. In consequence, a single column system is not recommended as it will be exposed to sudden unexpected bending forces that may cause the beam to suddenly fail, hence a double-column system is the next best option cost-effective wise since it will provide enough stability to compensate the bending effort without compromising the stability of the structure. Its placement, nevertheless, will be on the edges of the light and dark grey areas depicted in Figure 7 (at 1 m from the side edge of the deck) for a more even distribution of the acting forces.

The compressive force acting on each of the columns will then be each of the reactions on the girder beam, which due to symmetry are both of 40 kN.

3.2.3 Simple cantilever bridge

Despite most of the cantilever bridges being built with the help of trusses to adequately distribute and balance the loads, on a span of 30 m that is very ineffective since the space required by both the support structures and the suspended middle part are very large. Therefore, a simple cantilever structure will be used:

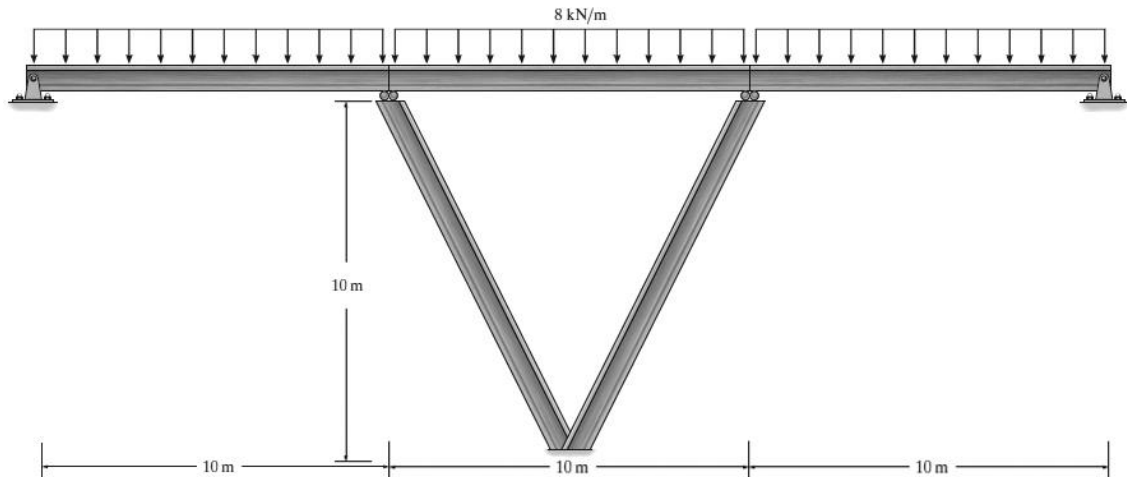


Figure 12. Simple cantilever bridge representation. (Jordi Mata Garcia, 2021)

As can be seen from Figure 12, the structure is in fact a double cantilever, each of the side loads balancing each other.

This structure offers the possibility of a single column base at the cost of the column beams taking not only pure compressive force as in the simply supported bridge but also bending stress created by the cantilever beam situation produced once the force is divided. Assuming again a double-column system, the 40 kN received from the girder beam will be divided as shown in Figure 13, rendering that $F_c = 35.78 \text{ kN}$ and $F_b = 17.89 \text{ kN}$, the latter creating a bending moment of $200 \text{ kN} \cdot \text{m}$ on the beam.

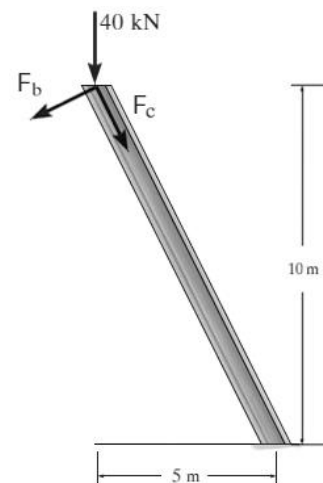


Figure 13. Cantilever column forces. (Jordi Mata Garcia, 2021)

3.2.4 Truss bridge

Truss bridges are likely one of the preferred options when it comes to short gaps due to their ease of assembly and their weight-carrying capabilities without the need for supports.

Despite the many different truss bridge designs, the Pratt truss was the one chosen for the initial design due to the critical components in the bridge being purely in compression and the possibility of below-deck clearance to keep things in the simplest of ways. The bridge will then be divided into 6 sections, two of them being triangular sections at each end of the bridge and $5\text{ m} \times 5\text{ m}$ square sections for the middle four sections with diagonal supports as described in Figure 14.

The reason for choosing squared sections is that having 45° angles on the diagonal beams help minimise the forces in both tension and compression members. Since modifying that angle decreases the forces in either the tension or compression members while increasing the opposite, the most optimal design to have the structure based on members under compression yet keeping it minimal is the chosen 45° angle.

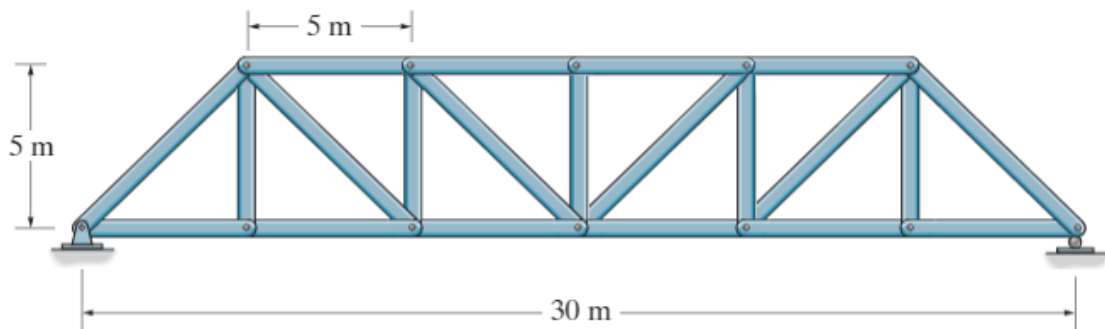


Figure 14. Pratt truss bridge design. (Jordi Mata Garcia, 2020)

Breaking down the forces inside the design following the traditional analysis results in:

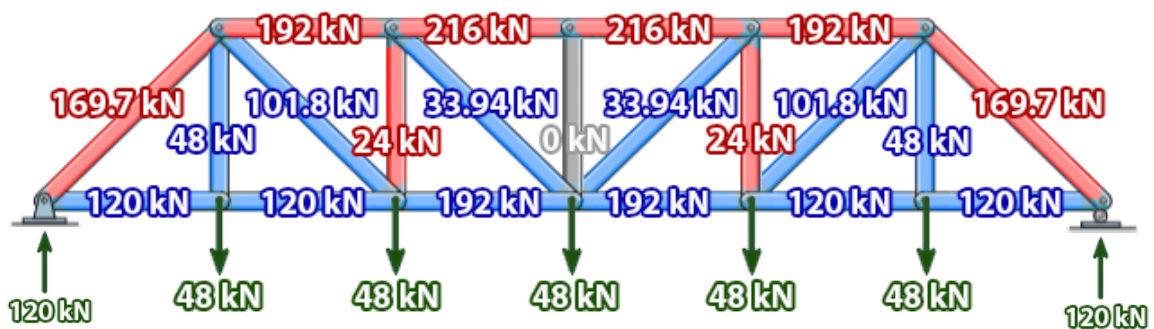


Figure 15. Pratt truss bridge design with forces. Red is compression, blue is tension. (Jordi Mata Garcia, 2020)

As observed in Figure 15, most of the longest members of the structure are kept under tensile load. This is beneficial as beams are prone to buckle under compressive forces, an effect that gets increased dramatically fast with the length of the member. Thus, upon initial inspection, the critical components to be studied will either be the end diagonal members under 169.7 kN of compressive force or the top members enduring 216 kN of compressive force.

It is important to note that this calculation is made assuming that the total load of 4 kN/m² is distributed evenly between each side of the truss and then acting solely on the joints. With the help of COMSOL software, it is possible to evaluate the effects of an evenly distributed load of 8 kN/m on the half truss structure analysed in Figure 15, observing that all the forces detailed in the figure get reduced by about 15%. For the sake of assuming the worst-case scenario, the forces detailed in Figure 13 will be taken as the ones acting in the structure.

3.2.5 Failure analysis applied to the critical components

According to the traditional calculations, the maximum bending stress σ_{max} [7, Eq. (6-12)] can be calculated according to:

$$\sigma_{max} = \frac{M_{Ed} \cdot c}{I} \quad (28)$$

where c is the distance from the neutral axis to the outermost side on the bending axis on the cross-section.

Similarly, the maximum shear stress τ_{max} caused by the shear force V_{Ed} [7, Eq. (7-3)] is obtained as follows:

$$\tau_{max} = \frac{V \cdot Q_{max}}{I \cdot t} \quad (29)$$

where Q_{max} is the maximum first moment of inertia of the cross-section.

Note: all the calculations will be made with the use of an Excel sheet where all the required calculations have been automated depending on loads, boundary conditions, cross-section profiles and steel category. Refer to Appendix E for more information.

3.2.5.1 Bridge deck – Central Beam

According to the values obtained in section 3.2.1 and using Equations 28 and 29, there is a possibility of evaluating the impact that M_{Ed} and V_{Ed} may have on the I-beam cross-section according to the IPE standards in terms of bending and shear stress based on a traditional stress analysis as shown in Table 9. It is easily observable that the limiting stress is the bending stress, which is an expected outcome when having a lengthy simply supported beam.

Table 9. Profile - stresses based on the traditional analysis. (Jordi Mata Garcia, 2021)

Profile	IPE220	IPE240	IPE270	IPE300	IPE330
σ_{max} [MPa]	396.83	308.33	233.16	179.51	140.19
τ_{max} [MPa]	42.90	37.18	31.15	26.18	22.53

There are many different steel categories depending mostly on its yielding stress, ranging from 235 MPa up to 450 MPa. For the sake of simplicity, the lesser yielding stress steel (S 235) will be assumed thus establishing the material's yielding stress at 235 MPa.

That assumption establishes, then, that IPE270 is the smallest profile that can be used since the maximum stress that it endures is barely below the yielding stress. If a certain safety margin is to be supposed, IPE330 is the next safest option since it is below 75% that of the yielding stress of the material.

However, when the maximum permitted deflection δ_{max} obtained from Figure 3 is compared to the limit condition deflection caused by a uniform distributed load on the beam δ_{Lim} as in Table 6:

$$\frac{\delta_{Lim_{IPE330}}}{\delta_{Max_{IPE330}}} \leq 1; \quad \frac{\delta_{Lim_{IPE330}}}{\delta_{Max_{IPE330}}} = \frac{\frac{5}{384} \cdot \frac{W \cdot L^4}{E \cdot I_y}}{L/400} = 1.69$$

The safety condition is failed; thus a different profile is needed. The smallest profile to satisfy that condition is the IPE400, hence the analysis will proceed with it.

Having it classified as a Class 1 cross-section the plastic analysis can be carried out on its own without any reduction affecting its resistance.

Through Equation 9 and Table 5 it is obtained that the design plastic shear resistance is $V_{c,Rd_{IPE400}} = 579.21 \text{ kN}$ and the moment capacity $M_{c,Rd_{IPE400}} = 307.15 \text{ kN} \cdot \text{m}$. Both values being bigger than the design values, it is confirmed that the beam will retain its full plastic capacities with ease.

As per the elastic critical moment, knowing that it is a simply supported beam with free ends and with a uniform distributed load applied on the top flange of the beam, it is obtained through Equation 20 that $M_{cr_{IPE400}} = 107.85 \text{ kN} \cdot \text{m}$. That value is greater than the design moment value M_{Ed} proving that the beam is indeed resistant to elastic deformation.

Finally, for the buckling resistance verification of the beam, there are two alternatives as specified in section “2.3.3.3 – Buckling resistance”: the method for I-shaped profiles or the general approach. If the method for I-shaped profiles is used, Equation 13 renders that $M_{b,Rd_{IPE400}} = 100 \text{ kN} \cdot \text{m}$. Despite that being deemed as safe per the method, when using the general approach it is obtained that $M_{b,Rd_{IPE400}} = 86.5 \text{ kN} \cdot \text{m}$, making it fail. This does not explicitly mean that the beam is unsafe as it fulfils the analysis dedicated exclusively for its profile shape. Yet, to guarantee maximum safety in the most critical component, the **IPE450** profile will be chosen as the definitive profile shape for all the beams present in the bridge deck component.

3.2.5.2 Simply supported bridge – Column

The main threat to a member that endures compressive forces, such as columns and pillars, is buckling failure. As per the traditional analysis, the elastic critical buckling stress N_{cr} can be obtained through Equation 21 while applying a certain effective length factor to the length of the member depending on the boundary conditions.

To serve as an example, a cantilevered beam would have a factor of $K = 2$. Using said values and knowing the column would sustain an axial load of $N_{Ed} = 40 \text{ kN}$, an IPE160 profile can endure a buckling force of $N_{cr_{IPE160}} = 45 \text{ kN}$ in its strong axis making it a good candidate to a reasonable extent.

Nonetheless, if proceeded with the Eurocode 3 safety conditions it is revealed through Equation 23 that this profile can only offer a total column strength of $N_{b,Rd_{IPE160}} = 13.38 \text{ kN}$, making it inadequate for safety.

The smallest profile that can offer an available column strength so that $N_{b,Rd} \geq N_{Ed}$ is an **IPE240**, with a total amount of $N_{b,Rd_{IPE240}} = 54.09 \text{ kN}$.

3.2.5.3 Simple cantilever bridge – Column

As in the previous situation, the column will withstand a vertical force coming from the girder of $F = 40 \text{ kN}$, yet as described in section “3.2.3 – Simple cantilever bridge” that force is divided into two components: an axial load of $N_{Ed} = 35.78 \text{ kN}$ and a bending point load of $P = 17.89 \text{ kN}$, the latter creating a shear force of $V_{Ed} = 17.89 \text{ kN}$ and a bending moment of $M_{Ed} = 200 \text{ kN} \cdot \text{m}$ at the base of the beam.

For the compressive part, the analysis proceeds in the same fashion as in the previous case yet considering that the length of the beam is now $L = 11.18 \text{ m}$. This agrees with the previous analysis, indicating that IPE240 is the smallest profile able to produce an available column strength greater than the axial load applied.

As per the buckling resistance, it is uttermost important to establish the alignment or orientation of the beam. If the bending moment happens on the strong axis y-y, the resistance of the beam will be several times higher than if the bending moment takes place along the weak axis z-z.

Just on the grounds of showing an example, the biggest IPE profile IPE600 will have a moment capacity of $M_{c,Rd_{IPE600}} = 825.32 \text{ kN} \cdot \text{m}$ on its strong axis but only of $M_{c,Rd_{IPE600}} = 114.12 \text{ kN} \cdot \text{m}$ on its weak axis, making it unsuitable to take the design moment of the beam. Similarly, the maximum deflection in the beam in its strong axis will be $\delta_{Max} = 0.0431 \text{ m}$ just under the limit deflection value $\delta_{Lim} = 0.0447$, meanwhile on its weak axis could reach $\delta_{Max} = 1.18 \text{ m}$.

Based on the maximum deflection of the beam, the only suitable profile is the **IPE600**, which will prove to be a suitable candidate by having a buckling resistance of $M_{b,Rd_{IPE600}} = 589.72 \text{ kN} \cdot \text{m}$. As observable, the limiting factor in this critical component is the deflection endured due to the bending moment more than the moment itself.

3.2.5.4 Truss Bridge – Members under compression

In the case of the truss bridge, there are two possible critical components:

1. Horizontal member: $N_{Ed_1} = 216 \text{ kN}$, $L_{o_1} = 5 \text{ m}$.
2. Diagonal member: $N_{Ed_2} = 169.7 \text{ kN}$, $L_{o_2} = 7.071 \text{ m}$.

For case number 1, the smallest profile that can endure N_{Ed_1} is IPE270 with an available column strength of $N_{b,Rd_1} = 282.61 \text{ kN}$.

For case number 2, the smallest profile that can endure N_{Ed_2} is IPE300 with an available column strength of $N_{b,Rd_1} = 214.67 \text{ kN}$.

As predicted, the diagonal members are the critical components in truss bridges. Thus, the **IPE300** profile will be the one used for the beams that make up the bridge.

3.2.6 Summary of beam profile selection according to Eurocode 3

Bridge deck:	<i>IPE450.</i>
Simply supported bridge column:	<i>IPE240.</i>
Simple cantilever bridge column:	<i>IPE600.</i>
Truss bridge members:	<i>IPE300.</i>

3.3 COMSOL Methodology

The COMSOL analyses will be performed using the Structural Mechanics module add-on.

A 3D stationary study will be performed on a multi-physics interface composed of a beam interface to act as the beam skeleton of the structure and a shell interface to act as the thin plate that carries the load applied to the structure. This will enable the “Multiphysics” interaction analysis, where “Shell-Beam” connections can be established over the shared edges of the beams and the thin plate with an offset established at half the height of the beam to indicate that the load of the thin plate is applied on the top flange of the beam.

In the study, it is very important to establish the correct orientation of the cross sections as the structures are designed according to the specifications of the I-beam profiles and using their strong axis. A wrong orientation may result in weaker structures.

As per the simulation of the deck beam interactions, a symmetry physics is applied to the joint between the longitudinal beams using axis 3 as the symmetry plane normal. Since a free end physics behaviour cannot be applied as the software does not accept an easy implantation of two beams resting on the same girder section, the symmetry physics allow the beams not to be continuous and thus creating wrong bending moments.

As a final note, since the software does not allow a roller support as a standard support system, a “prescribed displacement” fixture is applied to one end of the bridge allowing the displacement only in the longitudinal direction of the beam to create the roller support effect.

4 RESULTS

All analyses were performed with an Extra-fine meshing to guarantee accurate results.

4.1 Bridge deck

An initial analysis using COMSOL standard of the critical component with an IPE450 cross-section profile under an edge load of $8kN/m$ with a pinned near end and roller-supported on the far end rendering $\sigma_{Max} = 70MPa$, $\tau_{Max} = 10.54 MPa$ and a deflection of $\delta_{Max} = 15.63 mm$, agreeing greatly with the results obtained in section 3.2.1 – Bridge deck design taking into consideration the cross-sectional properties of the beam.

When analysing the whole bridge deck, a thin plate of $10 mm$ of the same steel S235 material will be used on top of the beams to simulate the beam flooring. This approach is not real since, in a real-life application, the deck would be a corrugated plate of very light metal, concrete or even a sandwich layered metal to serve as the base for the pavement, yet the weight carried by the plate to the beams is enough to produce a realistic dead load.

Nevertheless, when the whole deck is simulated taking into consideration the weight of the component members the values in the same critical member are modified, rendering a maximum deflection of $\delta_{Max} = 9.90 mm$, a maximum bending of $M_{Max} = 65.7 kN \cdot m$ and a maximum shear force of $V_{Max} = 19.73 kN$. Upon inspecting the stresses in the same element, a slight increase is appreciated in the normal stress appreciated where $\sigma_{Max} = 76.13MPa$ meanwhile, on the other hand, the shear stress halved its value for $\tau_{Max} = 5.30 MPa$. This is due to not only the effect of gravity on the members but also the interaction between the members creating an axial load in the members.

Also, as seen in the same Figure as the natural deflection of the plate also creates torsion in the side members as depicted in Figure 16, generating a lateral displacement of $10 mm$. This will create some warping stress on the side members, represented through the first principal stress in Figure 17. It can be observable in Figures 18 (Normal Stress) and 19 (von Mises stress), though, that the central beam is still the critical component.

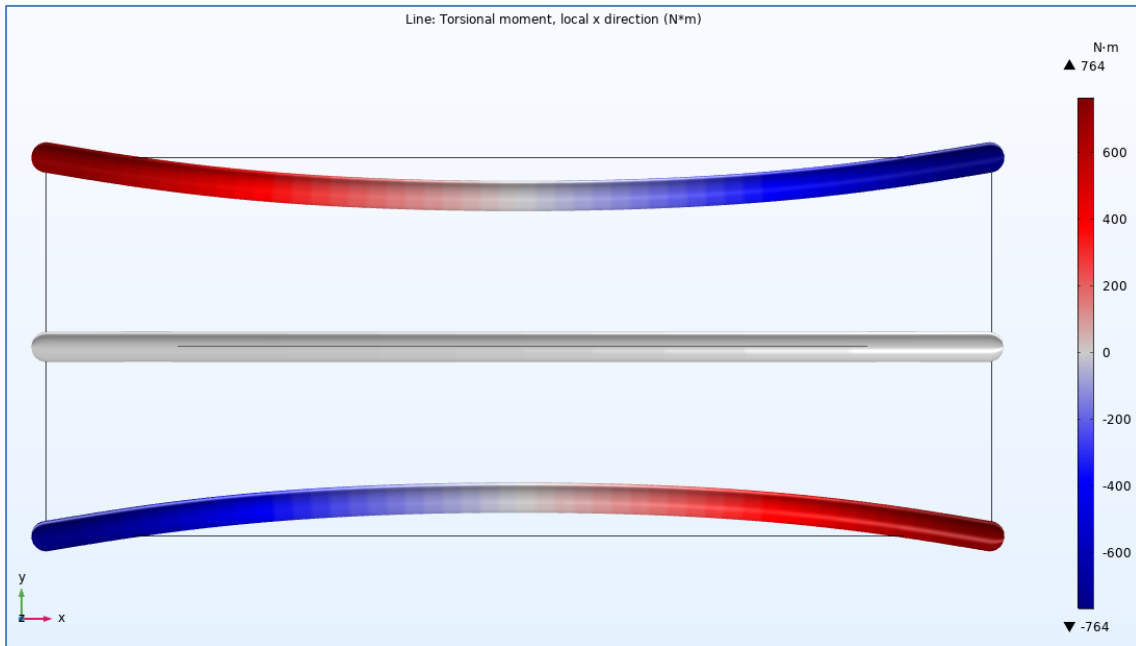


Figure 16. Bridge deck - Torsional moment analysis in COMSOL. (Jordi Mata Garcia, 2021)

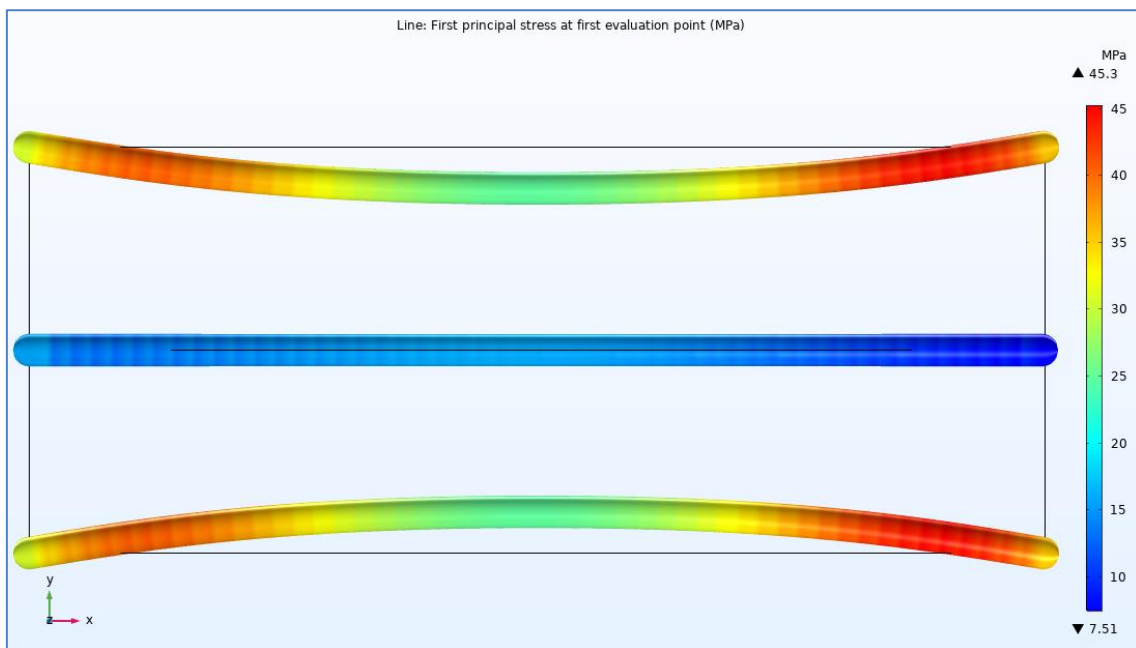


Figure 17. Bridge deck – first principal stress analysis in COMSOL (Jordi Mata Garcia, 2021).

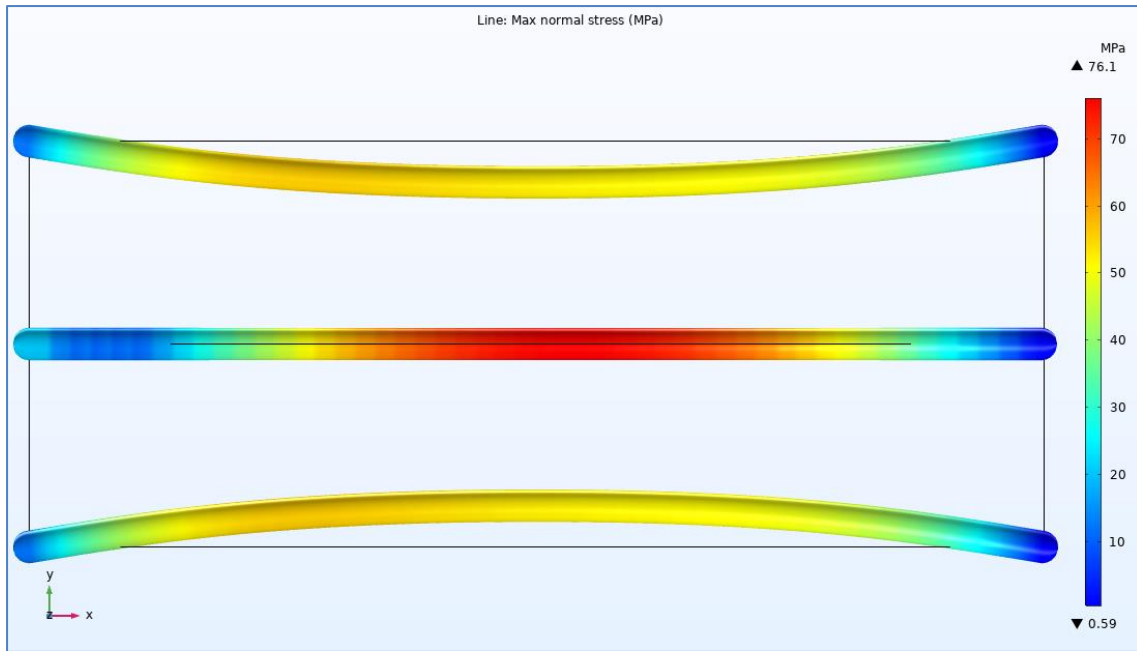


Figure 18. Bridge deck - Normal stress analysis in COMSOL (Jordi Mata Garcia, 2021).

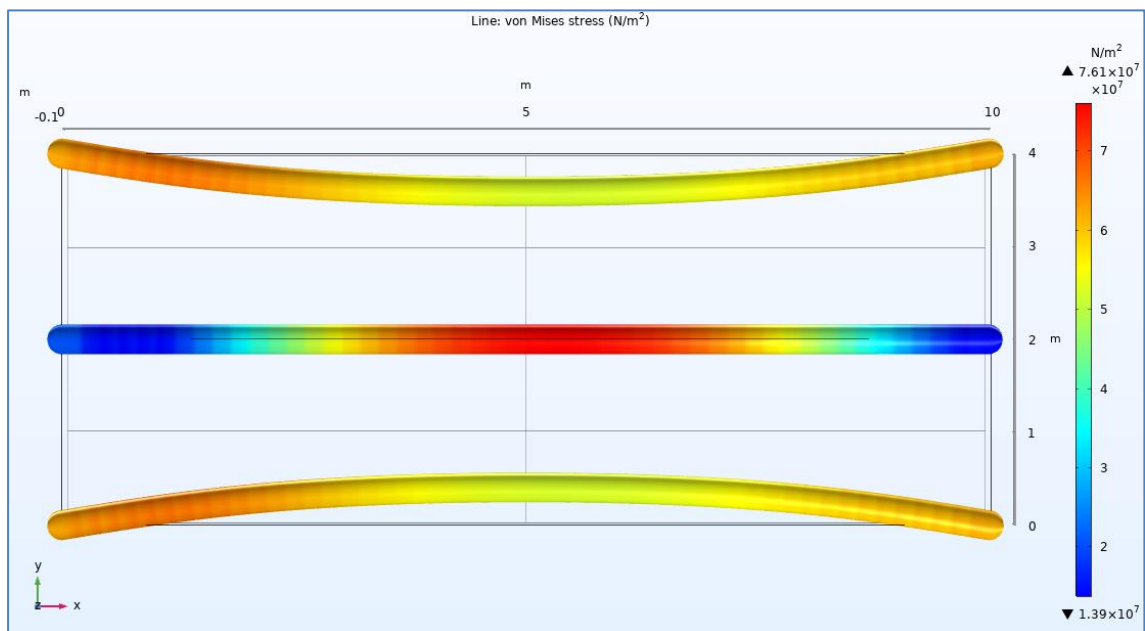


Figure 19. Bridge deck - von Mises stress analysis in COMSOL (Jordi Mata Garcia, 2021).

4.2 Simple bridge

The simulation of an individual support beam shows an evenly spread axial force load equal to the input thus adding no information to the situation.

In an ideal situation, due to the even load from both sides as the spans are both equal in shape and load the only force the column will endure is a vertical load as seen in Figure 20. In a more realistic approach, small lateral bending can occur due to the live load crossing the bridge. To simulate such a situation, the bridge structure can be simulated having the central span with a slightly higher load so each column section has to bend and warp, as seen in Figure 21.

The structure shows no big change, except on an increase of the von Mises stress especially on the joints of the side beams, indicating the shear stress to be the main cause of possible failure. The central beam seems to remain stable, most likely due to the whole deck structure balancing its stresses out. The appearance of such a small torsion moment in the column section indicates that the structure is very stable despite the live load location.

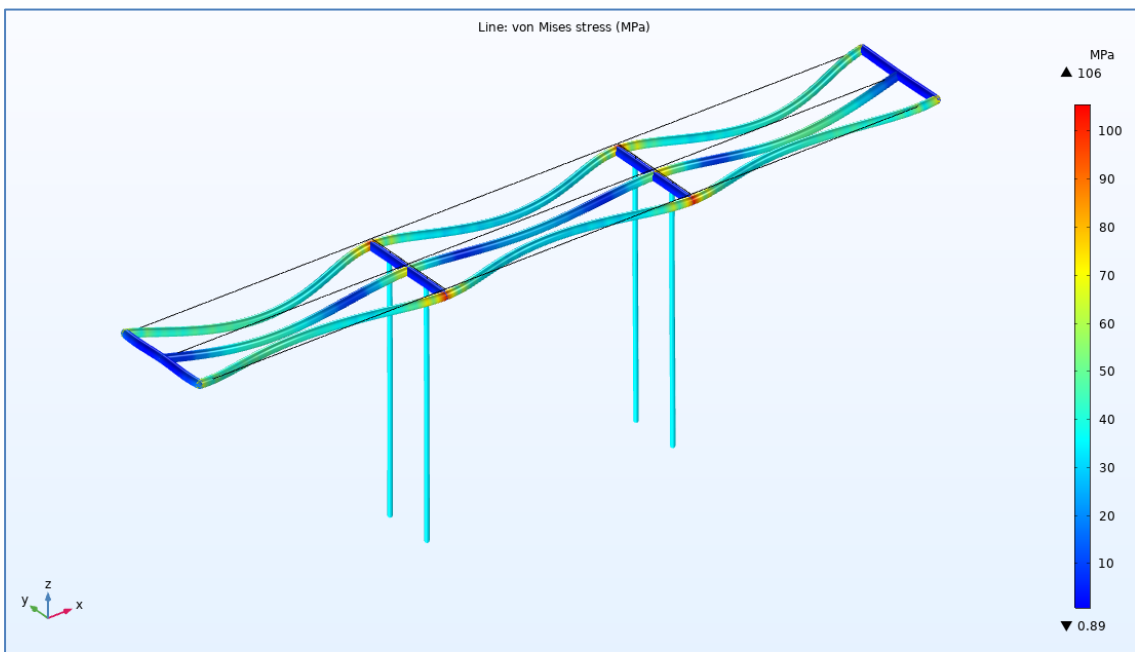


Figure 20. Simply supported bridge - whole structure von Mises stress analysis with equal loads in COMSOL. Deformation scaled by 150x. (Jordi Mata Garcia, 2021)

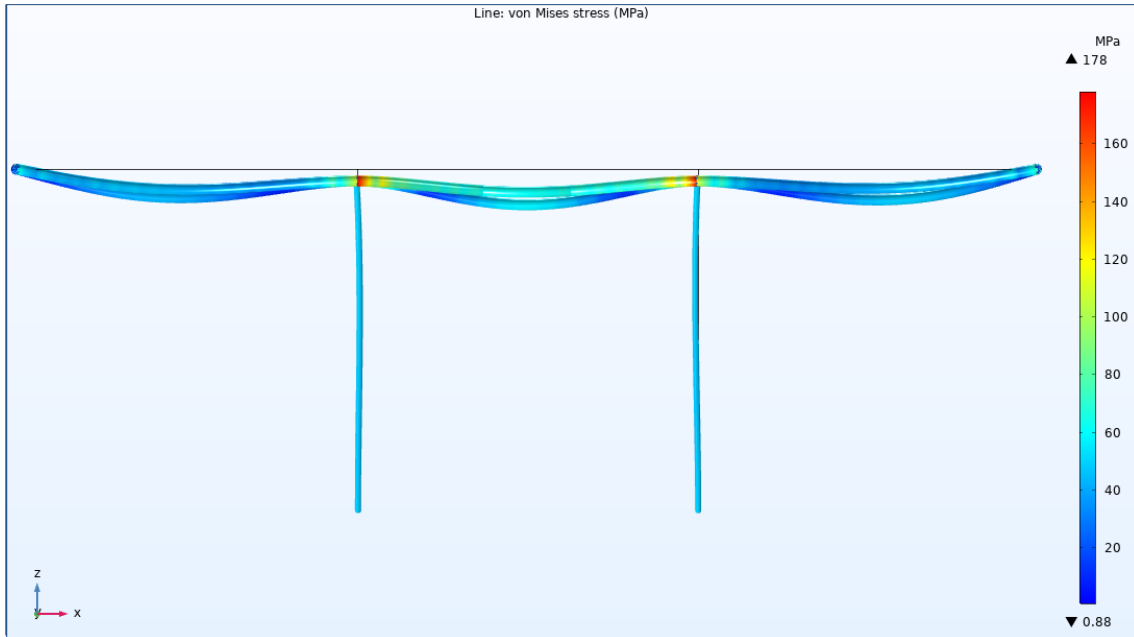


Figure 21. Bridge deck - whole structure von Mises stress analysis with middle-span load increased by 1.5x in COMSOL. Deformation scaled by 150x. (Jordi Mata Garcia, 2021)

There is an increase, though, in the axial load sustained by the columns due to the consideration of the dead load of the structure itself. The increase is, though, not substantial, and the now 86 kN are easily sustained by the strong axis of the column, which has an actual strength capacity of around 760 kN. The weak axis of the column would only sustain the possible rocking of the deck and could be easily addressed through the addition of a cement structure around the beam, bracing along the column section or increasing the cross-section size on the beam. Nonetheless, the profile will stay the same.

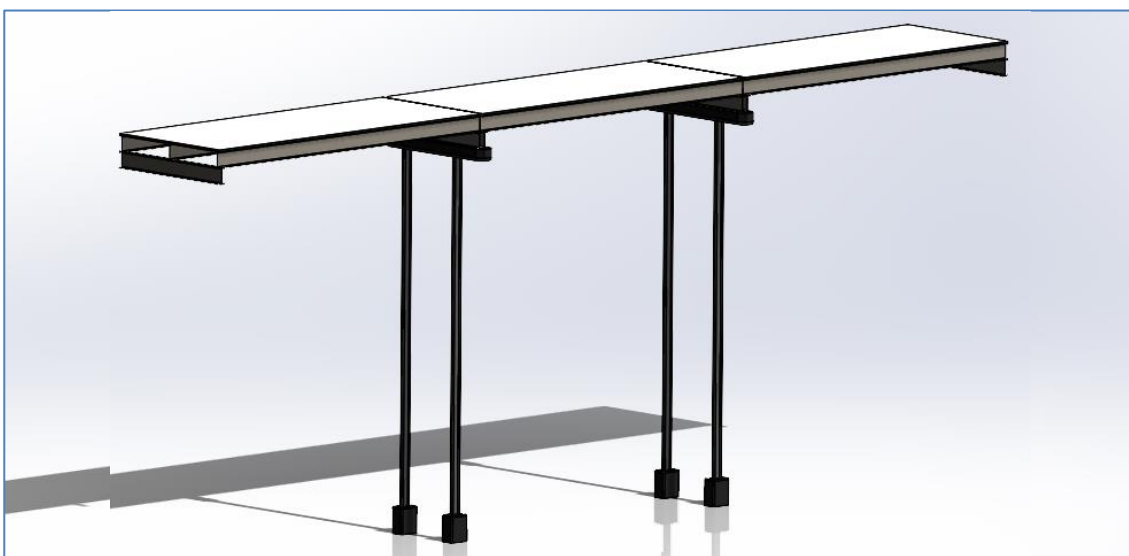


Figure 22. Simply supported bridge. (Jordi Mata Garcia, 2021)

4.3 Simple cantilever bridge

In a similar way as to the simply supported bridge, the addition of gravity increases the axial load in the support section of the bridge. In this instance, though, the much bigger cross-section takes the change with little to no effect.

It is also observable, as shown in Figure 23, that the deck structure and support pinning at the “cantilevered” end of the column prevents most of the bending caused in the column which was the critical reason for the choosing of the IPE600 cross-section profile. It could be optimised and reduced according to the simulation inputs; still, it is wisest to stick to the Eurocode 3 safety measures, thus the chosen profile will stay.

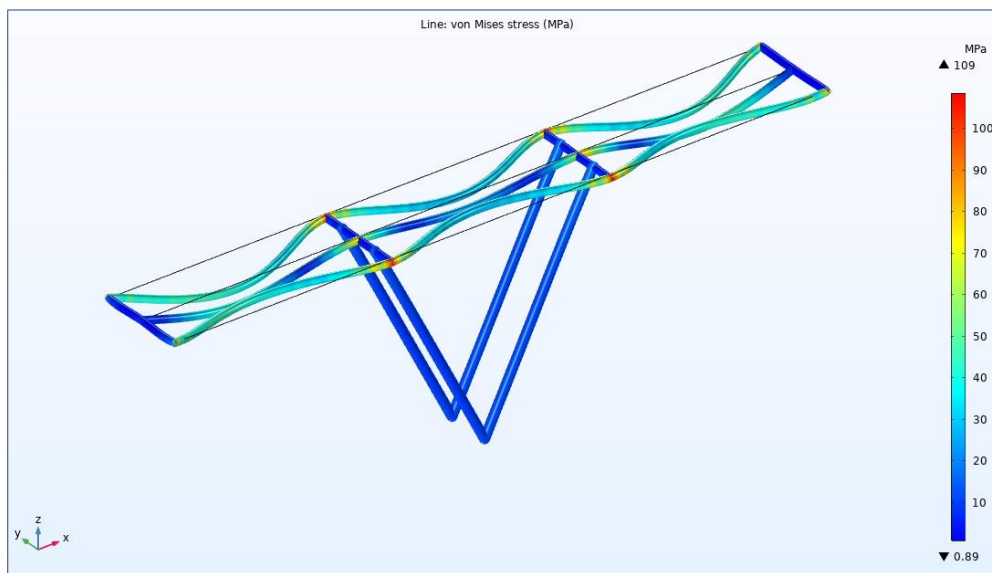


Figure 23. Simple cantilever bridge - whole structure von Mises stress analysis with equal loads. Deformation scaled by 200x. (Jordi Mata Garcia, 2021)

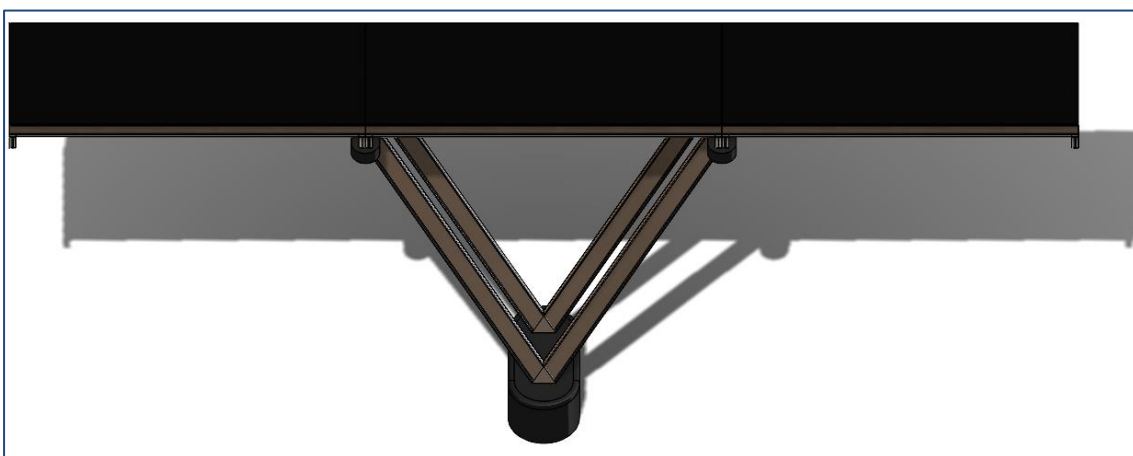


Figure 24. Simple cantilever bridge. (Jordi Mata Garcia, 2021)

4.4 Truss bridge

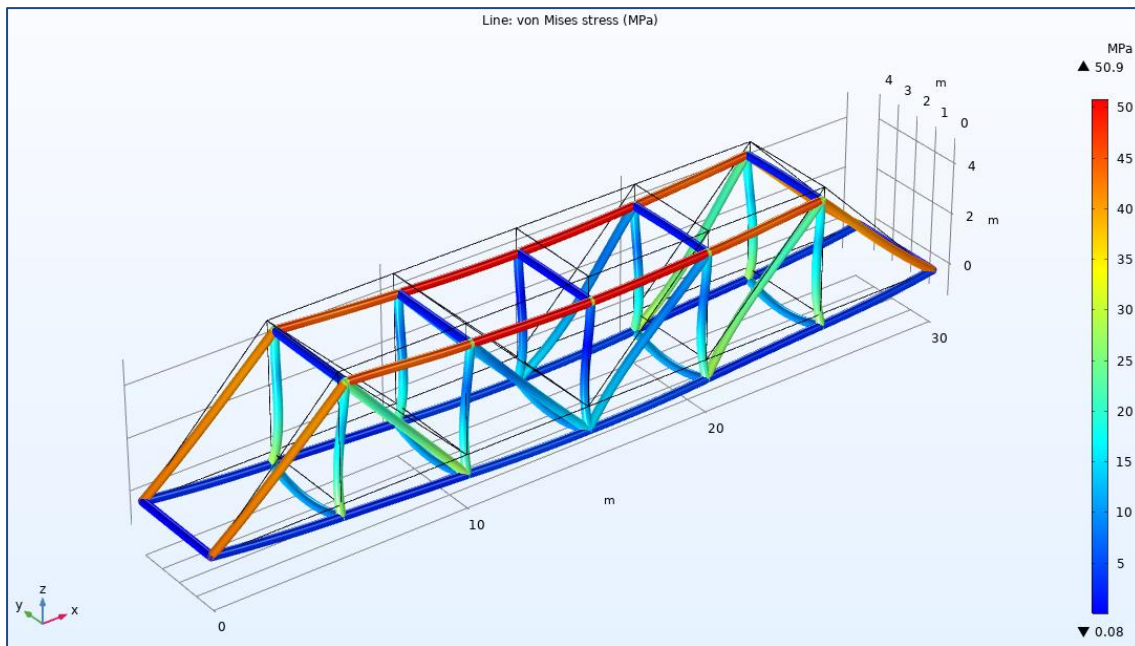


Figure 25. Truss bridge von Mises analysis in COMSOL. (Jordi Mata Garcia, 2021)

Due to the effect of gravity, it becomes apparent that the critical component of the truss structure has morphed from the diagonal starting element to the middle section top beam as seen in Figure 25. This is due to the effect of gravity pushing all the forces more to the centre. It is also remarkable that all the components under the heaviest stress are the members in compression, thus proving this bridge to be very adequate for the initial purpose of this analysis.

The axial load acting on the central beam has been increased from 216 kN to 268 kN , yet the beam's available strength is 393 kN thus providing more than enough room for that change to happen without compromising the integrity of the bridge.

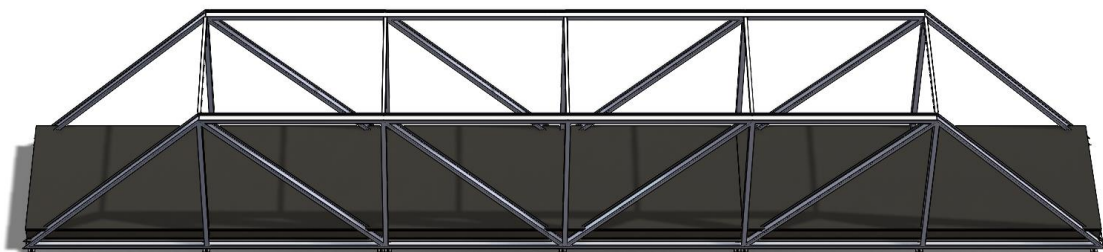


Figure 26. Truss bridge. (Jordi Mata Garcia, 2021)

4.5 Result comparison on minimum beam profiles

Table 10. Result comparison on minimum beam profiles between Eurocode 3 and COMSOL.

Eurocode 3	IPE	Max Stress	Factor of Safety
Bridge deck – Central beam	IPE450	76.1 MPa	3.1
Simply supported bridge - Column	IPE240	82 MPa	2.8
Simple cantilever bridge - Column	IPE600	13.3 MPa	17.7
Truss – Critical beam	IPE300	50.6 MPa	3.1
COMSOL			
Bridge deck – Central beam	IPE450	76.1 MPa	3.1
Simply supported bridge - Column	IPE300	33.5 MPa	7.0
Simple cantilever bridge - Column	IPE450	47.6 MPa	4.94
Truss – Critical beam	IPE300	50.6 MPa	3.1

5 DISCUSSION

5.1 Limitations

The findings of these studies have to be seen in the light of some limitations. The software tools used for the analyses were licensed as student version, thus removing many of the software capabilities. In the case of the SolidWorks software, the student version only includes very basic simulation tools where assemblies could not be analysed and supports could only be fixed, hence the entirety of the structure could only be analysed by incorporating it into a single combined part. This created many issues with the meshing at the intersection of the beams due to their filleted I shape that could only be solved by simplifying the joints as a “block”, thus creating small interferences in the production of the result. This also resulted in extra time used only in the refining of the structure to avoid the meshing process taking excessive long times due to the software being unable to specify what parts of the structure were causing problems since it could only refer to the entire combined body.

Furthermore, SolidWorks could only produce von Mises stress and displacement analyses on the designated structures. This, despite providing a great deal of information, was a setback since most of the times the reaction between elements and moments produced in their different axes were needed to be able to confirm the correct simulation or to address some of the potential issues.

Fortunately, due to the combined capabilities of COMSOL and SolidWorks, the structures could be simplified enough, as its individual required components analysed to obtain an adequate idea of the critical component's behaviour.

Still, it is difficult to establish the real impact on the whole combined structure as only estimations can be done on the propagating forces due to some lacking features in both software applications due to their licensing.

Concerning a more refined and accurate bridge selection, further analyses had to be considered concerning mode analysis. These analyses are very defined for the bridge structure type and would require a study that goes beyond the limits of this document as to the resistance of the structure to resonating frequencies and step excitation, the type of fastening and joints between members, amongst many others. The study is constrained to beam structural analysis and structural interaction between them.

5.2 Bridge deck

The analyses revealed the forces drawn from the initial analysis to be greater than those present in the beam once in the structure. Thus, even though the possibility of choosing a smaller profile accordingly, the IPE450 is the safest profile to choose to ensure the structure's proper stability.

Stability could be further improved by adding smaller beams in-between the main beams and specially girders to reduce the amount of torsion and bending taking place in the structure. That could help to further reduce the size of the main profiles, yet the weight of the bridge would increase exponentially. For the sake of simplicity, the design of the deck will remain as discussed.

The total weight of the bridge deck is 6398.12 *kg*, using a total of 0.82 *m*³ of steel.

5.3 Simply supported bridge

From the combination of analyses, there can be a discussion about the columns being able to safely support the final combined load. According to a strict interpretation of the Eurocode 3 safety analysis, the columns are in fact not able to withstand the axial load safely as the weak axis has an available strength of 54 kN , almost 30 kN less than the actual axial load.

The discussion is, then, what effects to take into consideration. As per the assumptions made, no increase in the profile is needed as there is no sideways rocking thus the only rocking sustained by the structure is placed on the strong axis. In a real-life application, the column would be reinforced to ensure stability or entirely replaced by a reinforced concrete structure as it is cheaper and reliable in this simple bridge applications.

In conclusion, if the safety condition is applied the beam should be replaced by an IPE300 beam to withstand the new axial load. Taking this profile as the final choice, each column would weigh 422.41 kg , not including joint and base structures.

The total final weight of the simply supported bridge is 20884 kg of S235 steel.

5.4 Simple cantilever bridge

In opposition to the simply supported bridge, the discussion would concern the possible reduction of the column profile. By understanding the actual behaviour of the beam and applying the Eurocode 3 standards, the profile will then be changed to an IPE450, hence resulting in an individual column weight of 845.2 kg .

The total final weight of the simple cantilever bridge is 22575.16 kg of S235 steel.

5.5 Truss bridge

The total volume of steel used by the truss bridge is 3.59 m^3 , resulting in a total of 28181.5 kg .

6 CONCLUSIONS

At first glance, the most cost-effective bridge option is the simply supported bridge, as even with the increased size of its column cross-section weights barely 20 tonnes, meaning cheapest materials. When compared to the cantilever bridge it does not show big flaws or differences other than the axial load reduction concerning the column section due to them being half the size in comparison and the placement of the base of the columns, which would make the bridges suitable for different scenarios in which there is an obstacle of any sort that forces the columns to be based only in the centre of the gap or anywhere but the centre.

The truss bridge clears the need for supports in the gap, which states why was it a very popular choice when having to cross deep gaps or bodies of water. It is also very robust, and the best-prepared choice to withstand transversal rocking motions. Still, it being as heavy can induce some problems on the base sections at the beginning and ending section of the bridge, making it unsuitable in the presence of not stable terrain, as observable by the analysis in Figure 25. When compared to 21 and 23, it is observable that the first two bridges have little to no load at the bridge entry and exit bases.

In conclusion, the lack of structural reasons other than best suitability for the required scenario proves the Eurocode 3 standard codebook to be an extremely powerful tool to design safe and lasting structures, as there was little to no need of changing the components specifications once the verifications were applied to the critical components after the finite element analyses were produced.

The COMSOL software tool was extremely useful in order to determine the interaction between the different elements on the structure. For example, in the case of the bridge deck it is very difficult to determine the extent of the torsion moment created due to the thin plate bending under the load and deforming the side beams. Thanks to COMSOL that warping can be quantized and properly evaluated as to whether the members can safely take those moments or not and to further optimise the structural members to be scored in an adequate range of safety as observed in Table 10.

REFERENCES

- [1] R. C. Hibbeler, Structural Analysis in SI Units, Harlow: Pearson Education Limited, 2019.
- [2] C. E. d. N. Eurocode 3: Basis of Structural Design., Brussels: EN 1990:2002+A1, 2005.
- [3] C. Bernuzzi and B. Cordova, Structural Steel Design to Eurocode 3 and AISC Specifications, Wiley, 2016.
- [4] P. C. Association, Handbook of frame constants: beam factors and moment coefficients for members of variable section, Chicago: Portland cement association, 1947.
- [5] C. E. d. N. Eurocode 1: Actions on Structures. Part 6: Traffic Loads on bridges, CEN, Brussels: EN 1991-2, 2008.
- [6] I. Baláž and Y. Koleková, “Safety Factors γ_{M0} and γ_{M1} in Metal Eurocodes,” in *21st International Conference ENGINEERING MECHANICS 2015*, Svratka, Czeck Republic, 2015.
- [7] R. C. Hibbeler, Mechanics of Materials 9th Edition (SI Edition), Pearson, 2014.

APPENDIX A

Fixed-End Moments Table

Fixed End Moments

<p> $(FEM)_{AB} = \frac{PL}{8}$ $(FEM)_{BA} = \frac{PL}{8}$ </p>	<p> $(FEM)'_{AB} = \frac{3PL}{16}$ </p>
<p> $(FEM)_{AB} = \frac{Pb^2a}{L^2}$ $(FEM)_{BA} = \frac{Pa^2b}{L^2}$ </p>	<p> $(FEM)'_{AB} = \left(\frac{P}{L^2}\right)\left(b^2a + \frac{a^2b}{2}\right)$ </p>
<p> $(FEM)_{AB} = \frac{2PL}{9}$ $(FEM)_{BA} = \frac{2PL}{9}$ </p>	<p> $(FEM)'_{AB} = \frac{PL}{3}$ </p>
<p> $(FEM)_{AB} = \frac{5PL}{16}$ $(FEM)_{BA} = \frac{5PL}{16}$ </p>	<p> $(FEM)'_{AB} = \frac{15PL}{32}$ </p>
<p> $(FEM)_{AB} = \frac{wL^2}{12}$ $(FEM)_{BA} = \frac{wL^2}{12}$ </p>	<p> $(FEM)'_{AB} = \frac{wL^2}{8}$ </p>
<p> $(FEM)_{AB} = \frac{11wL^2}{192}$ $(FEM)_{BA} = \frac{5wL^2}{192}$ </p>	<p> $(FEM)'_{AB} = \frac{9wL^2}{128}$ </p>
<p> $(FEM)_{AB} = \frac{wL^2}{20}$ $(FEM)_{BA} = \frac{wL^2}{30}$ </p>	<p> $(FEM)'_{AB} = \frac{wL^2}{15}$ </p>
<p> $(FEM)_{AB} = \frac{5wL^2}{96}$ $(FEM)_{BA} = \frac{5wL^2}{96}$ </p>	<p> $(FEM)'_{AB} = \frac{5wL^2}{64}$ </p>
<p> $(FEM)_{AB} = \frac{6EI\Delta}{L^2}$ $(FEM)_{BA} = \frac{6EI\Delta}{L^2}$ </p>	<p> $(FEM)'_{AB} = \frac{3EI\Delta}{L^2}$ </p>

APPENDIX B

Design properties of IPE profiles according to Eurocode 3

Profile	Depth	Width	Web thickness	Flange thickness	Root radius	Weight	Area	Second moment of area	Elastic section modulus	Plastic section modulus	Second moment of area	Torsion constant	Warping constant
	h [mm]	b [mm]	t _w [mm]	t _f [mm]	r [mm]	m [kg/m]	A [mm ²]	I _y [$\times 10^8$ mm ⁴]	W _{el,y} [$\times 10^3$ mm ³]	W _{pl,y} [$\times 10^3$ mm ³]	I _z [$\times 10^8$ mm ⁴]	I _t [$\times 10^6$ mm ⁴]	I _w [$\times 10^8$ mm ⁶]
IPE80	80	46	3.8	5.2	5	6	764	0.8014	20.03	23.22	0.08489	6.727	115.1
IPE100	100	55	4.1	5.7	7	8.1	1032	1.71	34.2	39.41	0.1592	11.53	342.1
IPE120	120	64	4.4	6.3	7	10.4	1321	3.178	52.96	60.73	0.2767	16.89	872
IPE140	140	73	4.7	6.9	7	12.9	1643	5.412	77.32	88.34	0.4492	24.01	1951
IPE160	160	82	5	7.4	9	15.8	2009	8.693	108.7	123.9	0.6831	35.3	3889
IPE180	180	91	5.3	8	9	18.8	2395	13.17	146.3	166.4	1.009	47.23	7322
IPE200	200	100	5.6	8.5	12	22.4	2848	19.43	194.3	220.6	1.424	68.46	12746
IPE220	220	110	5.9	9.2	12	26.2	3337	27.72	252	285.4	2.049	89.82	22310
IPE240	240	120	6.2	9.8	15	30.7	3912	38.92	324.3	366.6	2.836	127.4	36680
IPE270	270	135	6.6	10.2	15	36.1	4595	57.9	428.9	484	4.199	157.1	69469
IPE300	300	150	7.1	10.7	15	42.2	5381	83.56	557.1	628.4	6.038	197.5	124260
IPE330	330	160	7.5	11.5	18	49.1	6261	117.7	713.1	804.3	7.881	275.9	196090
IPE360	360	170	8	12.7	18	57.1	7273	162.7	903.6	1019	10.43	370.8	309370
IPE400	400	180	8.6	13.5	21	66.3	8446	231.3	1156	1307	13.18	504.1	482890
IPE450	450	190	9.4	14.6	21	77.6	9882	337.4	1500	1702	16.76	660.5	780970
IPE500	500	200	10.2	16	21	90.7	11552	482	1928	2194	21.42	886.2	1235400
IPE550	550	210	11.1	17.2	24	105.5	13442	671.2	2441	2787	26.68	1217	1861500
IPE600	600	220	12	19	24	122.4	15598	920.8	3069	3512	33.87	1646	2814700

Density:
 $\rho = 7850 \text{ kg/m}^3$ (= 490 lb/ft³)

Poisson's coefficient:
 $\nu = 0.3$

Longitudinal (Young's) modulus of elasticity:
 $E = 210\,000 \text{ N/mm}^2$ (= 30\,460 ksi)

Shear modulus:
 $G = \frac{E}{2(1+\nu)}$

Coefficient of linear thermal expansion:
 $\alpha = 12 \times 10^{-6} \text{ per } ^\circ\text{C}$ (= $6.7 \times 10^{-6} \text{ per } ^\circ\text{F}$)

Figure B1 & B2. Properties of IPE cross-sections and steel material. [3, Table 1.1]

Tab. 1: Recommended values of partial safety factors γ_{M0} and γ_{M1} in all 20 parts of EN 1993

EN 1993	-1-1	-1-2	-1-3	-1-4	-1-5	-1-6
γ_{M0}	1,0	ref. to -1-1	1,0	1,1	A.P.	A.P.
γ_{M1}	1,0	ref. to -1-1	1,0	1,1	A.P.	A.P.
EN 1993	-1-7	-1-8	-1-9	-1-10	-1-11	-1-12
γ_{M0}	A.P.	ref. to -1-1	-	-	-	-
γ_{M1}	A.P.	ref. to -1-1	-	-	-	-
EN 1993	-2	-3-1	-3-2	-4-1	-4-2	-4-3
γ_{M0}	1,0	1,0	1,0	1,0	1,0	-
γ_{M1}	1,1	1,0	1,1	1,1	1,1	-
EN 1993	-5	-6	Key:			
γ_{M0}	ref. to -1-1	1,0	ref. to -1-1 = refers to EN 1993-1-1			
γ_{M1}	ref. to -1-1	1,0	A.P. = as in relevant application part of EN 1993			

Figure B3. [6]

APPENDIX C

Shear Areas

- Rolled I- and H- shaped sections, with load parallel to the web:

$$A_v = A - 2bt_f + (t_w + 2r)t_f$$

Rolled channel sections, with load parallel to the web:

$$A_v = A - 2bt_f + (t_w + r)t_f$$

- Rolled T-shaped section, with load parallel to the web:

$$A_v = A - bt_f + (t_w + 2r)t_f/2$$

- Welded T-shaped section, with load parallel to the web:

$$A_v = t_w(h - t_f/2)$$

- Welded I-, H-shaped and box sections, with load parallel to the web:

$$A_v = \eta \sum (h_w t_w)$$

- Welded I-, H-shaped, channel and box sections, with load parallel to the flanges:

$$A_v = A - \sum (h_w t_w)$$

- Rolled rectangular hollow sections of uniform thickness with load parallel to the depth:

$$A_v = A \cdot h/(b + h)$$

- Rolled rectangular hollow sections of uniform thickness with load parallel to the width:

$$A_v = A \cdot b/(b + h)$$

- Circular hollow sections and tubes of uniform thickness:

$$A_v = 2A/\pi$$

where A is the cross-section area, b and h are the overall width and depth, respectively, h_w is the depth of the web, r is the root radius, t is the thickness (always take minimum value in case of not constant web thickness) and subscripts f and w are related to the flange and the web, respectively. Coefficient η is defined in EN 1993-1-5, recommending $\eta = 1.2$ for S235 to S460 steel grades and $\eta = 1.0$ for the rest, though it can be conservatively assumed equal to unity. [3, pp. 187-188]

APPENDIX D

Excel Spreadsheets

Steel	t ≤ 40 mm		40 mm ≤ t ≤ 80 mm		Steel data				Used Values				
	f _y [MPa]	f _u	f _y	f _u	ρ [kg/m ³]	v	E [GPa]	G	α [1/°C]	ε	f _y [MPa]	f _u	γ _{m0}
S 235	235	360	215	360	7850	0.3	210	80.76923	1.20E-05	1	235	360	1
Profile	r	h	b	s	t	A	A _v	I _y	I _z	I _t	I _w	W _{el,y}	W _{pl,y}
IPE450	21	450	190	9.4	14.6	9882	5085	337.4	16.76	660.5	780970	1500	1702
Bending	Class			Load at span		Span L		Max deflection		Ved		Med	
Flange	4.74657534 1			8 kN/m		10 m		0.025 m		40 kN		100 kNm	
Web	40.2978723 1									f		0.014702 m	
Section	1			GENERAL APPROACH				Buckling curve:		b		V _{c,Rd} 689.9191 kN	
Values for critical moment				λ _{LT} 1.690562								M _{c,Rd} 399.97 kNm	
k _z	1			α _{LT} 0.34								f _p 0.025 m	
k _w	1			Φ _{LT} 2.182396								(V _c /V _{c,Rd}) < 0.5 No influence	
C1	1.132			χ _{LT} 0.280697 ≤ 1? TRUE								(M _{ed} /M _{c,Rd}) < 1 No influence	
C2	0.459			M _{b,Rd} 112.2704 kNm				M _{b,Rd} ≥ Med		Safe		f/f _p ≤ 1 Permitted	
C3	0.525												
z _g	225			I- or H- SHAPED PROFILES APPROACH				Buckling curve:		c			
kc	0.77			M _{cr} 139.9475 kNm									
M _{cr}	139.947451 kNm			λ _{LT} 1.690562									
				α _{LT} 0.49									
				Φ _{LT} 1.887938									
				χ _{LT} 0.324684 ≤ 1? TRUE									
				f 1.067413 ≤ 1? FALSE									
				χ _{LT,mod} 0.304179									
				M _{b,Rd} 129.8639 kNm				M _{b,Rd} ≥ Med		Safe			

Figure D1. Eurocode 3 verification spreadsheet for bending with evenly spaced loads. (Jordi Mata Garcia, 2021)

Steel	t ≤ 40 mm		40 mm ≤ t ≤ 80 mm		Steel data				Used Values				
	f _y [MPa]	f _u	f _y	f _u	ρ [kg/m ³]	v	E [GPa]	G	α [1/°C]	ε	f _y [MPa]	f _u	γ _{m0}
S 235	235	360	215	360	7850	0.3	210	80.76923	1.20E-05	1	235	360	1
Profile	r	h	b	s	t	A	A _v	I _y	I _z	I _t	I _w	W _{el,y}	W _{pl,y}
IPE600	24	600	220	12	19	15598	8378	920.8	33.87	1646	2814700	3069	3512
Compression	Class			Unbraced lengths		Stability Curve		A _{eff}		ψ		k _σ	
Flange	4.210526 1			L _{o,y} 10 m		y a		14649.77		1		4	
Web	42.83333 4			L _{o,z} 10 m		z b		λ _p 0.754108		≤ 0.673		A=A	
Section	4			A= 14649.77				ρ 0.939208					
Elastic critical buckling stress				Imperfection factor		Relative slenderness		Reduction factor coefficient		Reduction factor			
N _{cr,y}	19084.66 kN			α _y 0.21		λ _y 0.424724		Φ _y 0.613791		χ _y 0.946159			
N _{cr,z}	701.9954 kN			α _z 0.34		λ _z 2.214534		Φ _z 3.29455		χ _z 0.174405			
F	40 kN			Available column strength		λ _y ≤ 2? FALSE		N _{ed} /N _{cr,y} ≤ 0.04? TRUE					
σ	2.730418 Mpa			N _{b,Rd} 600.4223 kN		λ _z ≤ 2? FALSE		N _{ed} /N _{cr,z} ≤ 0.04? FALSE					
										Can buckling be neglected for axis y?		TRUE	
										Can buckling be neglected for axis z?		FALSE	

Figure D2. Eurocode 3 verification spreadsheet for members in compression. (Jordi Mata Garcia, 2021)

Steel	$t \leq 40 \text{ mm}$		$40 \text{ mm} < t \leq 80 \text{ mm}$		Steel data					Used Values				
	f_y [MPa]	f_u	f_y	f_u	ρ [kg/m ³]	ν	E[GPa]	G	α [1/°C]	ϵ	f_y [MPa]	f_u	γ_{m0}	
S 235	235	360	215	360	7850	0.3	210	80.76923	1.20E-05	1	235	360	1	
Profile	r	h	b	s	t	A	Av	ly	lz	lt	lw	W _{el,y}	W _{pl,y}	
IPE450	21	450	190		9.4	14.6	9882	5085	337.4	16.76	660.5	780970	1500	1702
Bending	Class		Load at cantilever end		Span L		Max deflection		Ved		Med			
Flange	4.74657534		17.89 kN		11.18 m		0.04472 m		40 kN		100 kNm			
Web	40.2978723								f		0.117612 m			
Section	1								V _{c,Rd}		689.9191 kN			
									M _{c,Rd}		399.97 kNm			
									f _p		0.04472 m			
									(V _{ed} /V _{c,Rd}) < 0.5		No influence			
									(M _{ed} /M _{c,Rd}) <= 1		No influence			
									f/f _p <= 1		NOT PERMITTED			
GENERAL APPROACH													Buckling curve:	b
Values for critical moment													λ_{LT}	1.791915
kz	1								α_{LT}		0.34			
kw	1								Φ_{LT}		2.376105			
C1	1.132								χ_{LT}		0.254031 <= 1? TRUE			
C2	0.459								M _{b,Rd}		101.6048 kNm			
C3	0.525								M _{b,Rd} >= Med		Safe			
z _g	225 <- Load on top flange								I- or H- SHAPED PROFILES APPROACH		Buckling curve:		c	
kc	0.77								M _{cr}		124.564 kNm			
									λ_{LT}		1.791915			
									α_{LT}		0.49			
									Φ_{LT}		2.045129			
									χ_{LT}		0.296106 <= 1? TRUE			
									f		1.111296 <= 1? FALSE			
									χ_{LT_mod}		0.266451			
									M _{b,Rd}		118.4335 kNm			
									M _{b,Rd} >= Med		Safe			

Figure D3. Eurocode 3 verification spreadsheet for bending in cantilevered beams. (Jordi Mata Garcia, 2021)

Pratt Truss of 6 sections				Traditional			COMSOL P			COMSOL Even		
				AB	169.7056	169.7056275	140					
				BC	192	192	160					
				CD	216	216	180					
				AG	120	120	100					
				GF	120	120	100					
				FE	192	192	160					
				BG	48	48	40					
				CF	24	24	20					
				DE	0	0	0					
				BF	101.8234	101.8233765	84.852					
				CE	33.94113	33.9411255	28.284					
Traditional Analysis												
A			G			B			F			
AB = 169.7056			GB = 48			BA = 169.7056			FG = 120			
AG = 120			GF = 120			BG = 48			FB = 101.8234			
			GA = 120			BF = 101.8234			FE = 192			
						BC = 192			FC = 24			
R _A = 120			P _G = 48						P _F = 48			
C			E			D						
CB = 192			EF = 192			DC = 216						
CF = 24			EC = 33.94113			DE = 0						
CE = 33.94113			ED = 0									
CD = 216			P _E = 48									

Figure D4. Truss structure calculator. (Jordi Mata Garcia, 2021)